Day versus night and the evolution of sexual dimorphism in Lepidoptera

Richard Rabideau Childers

rchilders@g.harvard.edu

Harvard University https://orcid.org/0000-0002-7137-3192

Wei-Ping Chan

Harvard University

Blake Dickson

Department of Anatomy, University of New South Wales

Sorcha Ashe

https://orcid.org/0000-0002-1757-0582

Liming Cai

Department of Integrative Biology, The University of Texas, Austin

James Crall

Harvard University https://orcid.org/0000-0002-8981-3782

Mark Cornwall

Harvard University

Even Dankowicz

Harvard University https://orcid.org/0000-0001-7202-8502

Jomar Hinolan

National Museum of the Philippines

Micael Itliong

City University of New York https://orcid.org/0000-0002-9222-6984

Crystal Maier

Harvard University

Sarah Maunsell

Harvard University

Wendy A. Valencia-Montoya

Department of Organismic and Evolutionary Biology and Museum of Comparative Zoology, Harvard University, Cambridge, Massachusetts, United States https://orcid.org/0000-0001-9246-2330

Avalon Owens

The Rowland Institute, Harvard University

Rachel Hawkins Sipe

Department of Organismic and Evolutionary Biology and Museum of Comparative Zoology, Harvard University

Mary Stoddard
Princeton University https://orcid.org/0000-0001-8264-3170

Anshuman Swain
Department of Ecology and Evolutionary Biology, University of Michigan

Gerard Talavera
CSIC https://orcid.org/0000-0003-1112-1345

João Tonini
University of Richmond https://orcid.org/0000-0002-4730-3805

Cheng-Chia Tsai
Columbia University https://orcid.org/0000-0001-5662-6908

Roger Vila
Institut de Biologia Evolutiva (CSIC-Universitat Pompeu Fabra) https://orcid.org/0000-0002-2447-4388

Kwaku Aduse-Poku
Howard University

Vijay Barve
University of Florida

Ana Paula Carvalho
McGuire Center for Lepidoptera and Biodiversity, Florida Museum of Natural History, University of Florida

Mark Arcebal Naive
University of Chinese Academy of Sciences

David Plotkin
Florida Museum of Natural History, University of Florida https://orcid.org/0000-0002-2339-655X

Vaughn Shirey
University of Florida

Andrei Sourakov
Florida Museum of Natural History https://orcid.org/0000-0002-7835-7232

Emmanuel Toussaint
Department of Entomology, Natural History Museum of Geneva

Marianne Espeland
Leibniz Institute for the Analysis of Biodiversity Change, Museum Koenig

Robert Guralnick
University of Florida

Walter Jetz
Yale University https://orcid.org/0000-0002-1971-7277

Akito Kawahara
University of Florida https://orcid.org/0000-0002-3724-4610

David Lohman
City College of New York https://orcid.org/0000-0002-0689-2906
Leslie Ries
Georgetown University
Gary Bernard
University of Washington https://orcid.org/0000-0001-7460-5123
Edward Soucy
Harvard University
Nanfang Yu
Columbia University https://orcid.org/0000-0002-9462-4724
Naomi Pierce
Harvard University https://orcid.org/0000-0003-3366-1625

Biological Sciences - Article

Keywords:

Posted Date: November 4th, 2025

DOI: https://doi.org/10.21203/rs.3.rs-7603116/v1

Additional Declarations: There is **NO** Competing Interest.

Day versus night and the evolution of sexual dimorphism in Lepidoptera

Authors: Richard Rabideau Childers[1,2]*†, Wei-Ping Chan[1,2]† , Blake V. Dickson[3], Sorcha Ashe[1,2], Liming Cai[4], James D. Crall[1,2,5], Mark A. Cornwall[1,2], Even Dankowicz[1,2], Jomar Hinolan[6], Micael Gabriel Itliong[7-8], Crystal A. Maier[2], Sarah Maunsell[1,2], Wendy A. Valencia-Montoya[1,2], Avalon C. S. Owens[9], Rachel Hawkins Sipe[2], Mary Caswell Stoddard[10], Anshuman Swain[2,11], Gerard Talavera[12], João Filipe R. Tonini[1,2,13], Cheng-Chia Tsai[14], Roger Vila[15], Kwaku Aduse-Poku[16] , Vijay Barve[17,18], Ana Paula S. Carvalho[17,19], Mark Arcebal K. Naive[20-21], David Plotkin[17,22], Vaughn Shirey[17,23], Andrei Sourakov[17], Emmanuel F.A. Toussaint[24], Marianne Espeland[25], Robert Guralnick[17,4], Leslie Ries[23], Walter Jetz[26,27], Akito K. Kawahara[17,22,4], David J. Lohman[28-30], Gary D. Bernard[31], Edward R. Soucy[32], Nanfang Yu[14], Naomi E. Pierce[1,2]*

†These authors contributed equally to this work. *To whom correspondence should be addressed.

1. Department of Organismic and Evolutionary Biology, Harvard University, Cambridge, MA 02138, USA
2. Museum of Comparative Zoology, Harvard University, Cambridge, MA 02138, USA
3. Department of Anatomy, University of New South Wales, Sydney, NSW 2033, Australia
4. Department of Biology, The University of Florida, Gainesville, Florida, 32611, USA
5. Department of Entomology, University of Wisconsin-Madison, WI, 53706, USA
6. Botany and National Herbarium Division, National Museum of the Philippines, Manila, Philippines.
7. Department of Biology, Polytechnic University of the Philippines, Sta. Mesa, 1016 Manila, Philippines
8. Initiatives for Conservation, Landscape Ecology, Bioprospecting, and Biomodeling (iCOLABB), Research Center for the Natural and Applied Sciences, University of Santo Tomas, España Blvd, Sampaloc, Manila 1008, Philippines
9. The Rowland Institute at Harvard, Harvard University, Cambridge, MA, 02138, USA
10. Department of Ecology & Evolutionary Biology, Princeton University, Princeton, NJ 08544, USA
11. Department of Ecology and Evolutionary Biology, University of Michigan, Ann Arbor, MI 48109, USA
12. Institut Botànic de Barcelona (IBB), CSIC-CMCNB, 08038 Barcelona, Catalonia, Spain
13. Department of Biology, University of Richmond, Richmond VA, 23173
14. Department of Applied Physics & Applied Math, Columbia University, New York, NY 10027
15. Institut de Biologia Evolutiva (CSIC-Univ. Pompeu Fabra), Barcelona, 08003, Spain
16. Department of Biology, Howard University, Washington DC 20059, USA
17. McGuire Center for Lepidoptera and Biodiversity, Florida Museum of Natural History, University of Florida, Gainesville, FL 32611
18. Natural History Museum of Los Angeles County, Los Angeles, California 90007 USA.

19. Department of Entomology, Smithsonian Institution, National Museum of Natural History, Washington, DC, 20560 USA.
20. Center for Integrative Conservation, Xishuangbanna Tropical Botanical Garden, Chinese Academy of Sciences, Mengla, Yunnan 666303, China
21. University of Chinese Academy of Sciences, Beijing 100049, China
22. Entomology and Nematology Department, University of Florida, Gainesville 32608, FL, USA
23. Department of Biology, Georgetown University, Washington, DC 20057, USA
24. Department of Entomology, Natural History Museum of Geneva, Geneva, Switzerland
25. Leibniz Institute for the Analysis of Biodiversity Change, Museum Koenig, Centre for Taxonomy and Morphology, Bonn, Germany
26. Department of Ecology & Evolutionary Biology, Yale University, New Haven, CT, USA
27. Center for Biodiversity and Global Change, Yale University, New Haven, CT, USA
28. Department of Biology, City College of New York, City University of New York, New York, NY 10031, USA
29. PhD Program in Biology, Graduate Center, City University of New York, New York, NY 10016, USA
30. Entomology Section, National Museum of Natural History, Manila, Philippines
31. Department of Electrical & Computer Engineering, University of Washington, Seattle, WA 98195, USA
32. Center for Brain Science, Harvard University, 52 Oxford St. Room 331, Cambridge, MA 02138, USA

ORCIDs/emails:

Richard Rabideau Childers*: 0000-0002-7137-3192; rchilders@g.harvard.edu

Wei-Ping Chan*:0000-0002-7132-9191; chanw@g.harvard.edu

Blake V. Dickson: 0000-0001-6299-5224; b.dickson@unsw.edu.au

Sorcha Ashe: 0000-0002-1757-0582; ashesorcha@gmail.com

Liming Cai: 0000-0002-8982-2435; lmcai@utexas.edu

James D. Crall: 0000-0002-8981-3782; james.crall@wisc.edu

Mark A. Cornwall: 0000-0003-2528-2561; mark.a.b.cornwall@gmail.com

Even Dankowicz: 0000-0001-7202-8502; edankowicz@gmail.com

Marianne Espeland: 0000-0002-6800-4783; m.espeland@leibniz-lib.de

Jomar Hinolan: 0000-0002-4446-3803; jomar.hinolan@nationalmuseum.gov.ph

Micael Gabriel Itliong: 0000-0002-9222-6984; imicaelgabriel@gmail.com

Crystal A. Maier: 0000-0001-6435-2775; cmaier@fas.harvard.edu

Sarah Maunsell: 0000-0003-1633-231X; sarahmaunsell01@gmail.com

Wendy A. Valencia-Montoya: 0000-0001-9246-2330 wvalenciamontoya@g.harvard.edu

Avalon C. S. Owens: 0000-0001-7212-2275; aowens@fas.harvard.edu

Rachel Hawkins Sipe: 0000-0002-2225-1084; rachelhawkins12@gmail.com

Mary Caswell Stoddard: 0000-0001-8264-3170 ; mstoddard@princeton.edu

Anshuman Swain: 0000-0002-9180-2222; answain@umich.edu

Gerard Talavera: 0000-0003-1112-1345; gerard.talavera@csic.es

João Filipe R. Tonini: 0000-0002-4730-3805; jtonini@richmond.edu

Cheng-Chia Tsai: 0000-0001-5662-6908; ct2443@columbia.edu

Roger Vila: 0000-0002-2447-4388; roger.vila@csic.es

Kwaku Aduse-Poku: 0000-0002-0158-9801; Kwaku.AdusePoku@howard.edu

Vijay Barve: 0000-0002-4852-2567; vijay.barve@gmail.com

Ana Paula S. Carvalho: 0000-0003-3245-3648; acarvalho@ufl.edu

Mark Arcebal K. Naive: 0000-0002-1548-9465; arciinaive19@gmail.com

David Plotkin: 0000-0002-2339-655X; dplotkin@ufl.edu

Vaughn Shirey: 0000-0002-3589-9699; vms55@georgetown.edu

Andrei Sourakov: 0000-0002-7835-7232; asourakov@flmnh.ufl.edu

Emmanuel F.A. Toussaint: 0000-0002-8439-1285; emmanuel.toussaint@geneve.ch

Robert Guralnick: 0000-0001-6682-1504; rguralnick@flmnh.ufl.edu

Walter Jetz: 0000-0002-1971-7277; walter.jetz@yale.edu

Akito K. Kawahara: 0000-0002-3724-4610; kawahara@flmnh.ufl.edu

David J. Lohman: 0000-0002-0689-2906; dlohman@ccny.cuny.edu

Leslie Ries: 0000-0002-5953-9284;leslie.ries@georgetown.edu

Gary D. Bernard: 0000-0001-7460-5123; garyber@u.washington.edu

Edward R. Soucy: 0000-0002-1187-5596; soucy@mcb.harvard.edu

Nanfang Yu: 0000-0002-9462-4724; ny2214@columbia.edu

Naomi E. Pierce: 0000-0003-3366-1625; npierce@oeb.harvard.edu

(200/200 words).

Many species exhibit consistent morphological differences between males and females. This sexual dimorphism sparked debate between Charles Darwin, who attributed it to sexual selection favoring

male traits that appeal to females, and Alfred Russell Wallace, who argued that natural selection favored cryptic traits in females to evade predators. Here, using multispectral imaging of wing reflectance and patterning across 274 butterfly and moth species sampled from recent phylogenetic frameworks, we demonstrate that Darwinian and Wallacean models both describe aspects of the evolution of lepidopteran coloration, with Darwinian sexual selection largely acting on visible male traits in diurnal species, while Wallacean natural selection tends to act on female traits of nocturnal species: In butterflies, wing reflectance and color pattern traits exhibit the strongest dimorphism in dorsal and forewing areas, areas predicted to experience strong sexual selection, with male traits evolving more quickly and exhibiting greater between-species disparity than those of females (indicators of sexual selection), but only in wavelengths perceptible to butterflies. In contrast, in nocturnal moths, evolutionary rate and disparity are strongly female biased. Ancestrally nocturnal geometrid moths, where diurnal behavior has evolved repeatedly, confirm this trend of male-biased rates and disparity in diurnal species, especially on dorsal and forewing surfaces.

Main text

On the origins of sexual dimorphism:

Males and females of many species look strikingly different. This has been studied in birds and butterflies, and sparked a debate between Charles Darwin, who proposed that such differences result from sexual selection for elaborate male traits, and Alfred Russel Wallace, who argued that sexual dimorphism stems from natural selection favoring females that are drab or cryptic as a defense against predation. Evidence supports both hypotheses in different animal taxa,[1–5] with much early attention focusing on butterflies[6–8]. Butterfly wing color and patterns serve various functions that vary in selective context, ranging from mate signaling to predator avoidance to abiotic tolerance. For instance, a recent macroevolutionary study on non-hesperiid European butterflies found strong support for Darwin's model, with faster male color evolution driving differences in male-female color dimorphism[6]. In contrast, ecological and predation pressure, as predicted by Wallace, have been found to be stronger drivers of sexual dimorphism in in swallowtail butterflies[7], while evidence for both Darwin's and Wallace's models was found in another recent study of birdwing butterflies, (family Papilionidae[9]).

However, much of this earlier work largely focused on the spectrum visible to humans, and rarely considered ultraviolet ('UV'; 100-400 nm) wavelengths[6,7,9,10], though see Reference 11). This omission is significant, as UV is not only perceptible to butterflies, but is actively involved in their sexual selection[12–15]. Further, two recent studies[16,17] on butterflies found that climate variables were more strongly associated with near-infrared ('NIR'; 700-1400 nm) than UV-visible (320-680 nm) reflectance. Sexual dimorphism, in contrast, was found only in UV-visible wavelengths[16], highlighting how distinct sections of the reflectance spectrum do not evolve uniformly, but instead are shaped by contrasting selective pressures. A comprehensive assessment of natural and sexual selective forces shaping butterfly color and pattern evolution must, therefore, account for the full gamut of signals across the electromagnetic (EM) spectrum, yet has remained elusive. Given the role that butterflies have played in our understanding of

evolutionary dynamics, they represent an ideal model system for assessing the relative importance of sexual vs. natural selection in driving sexual dimorphism throughout the visual and non-visual spectrum.

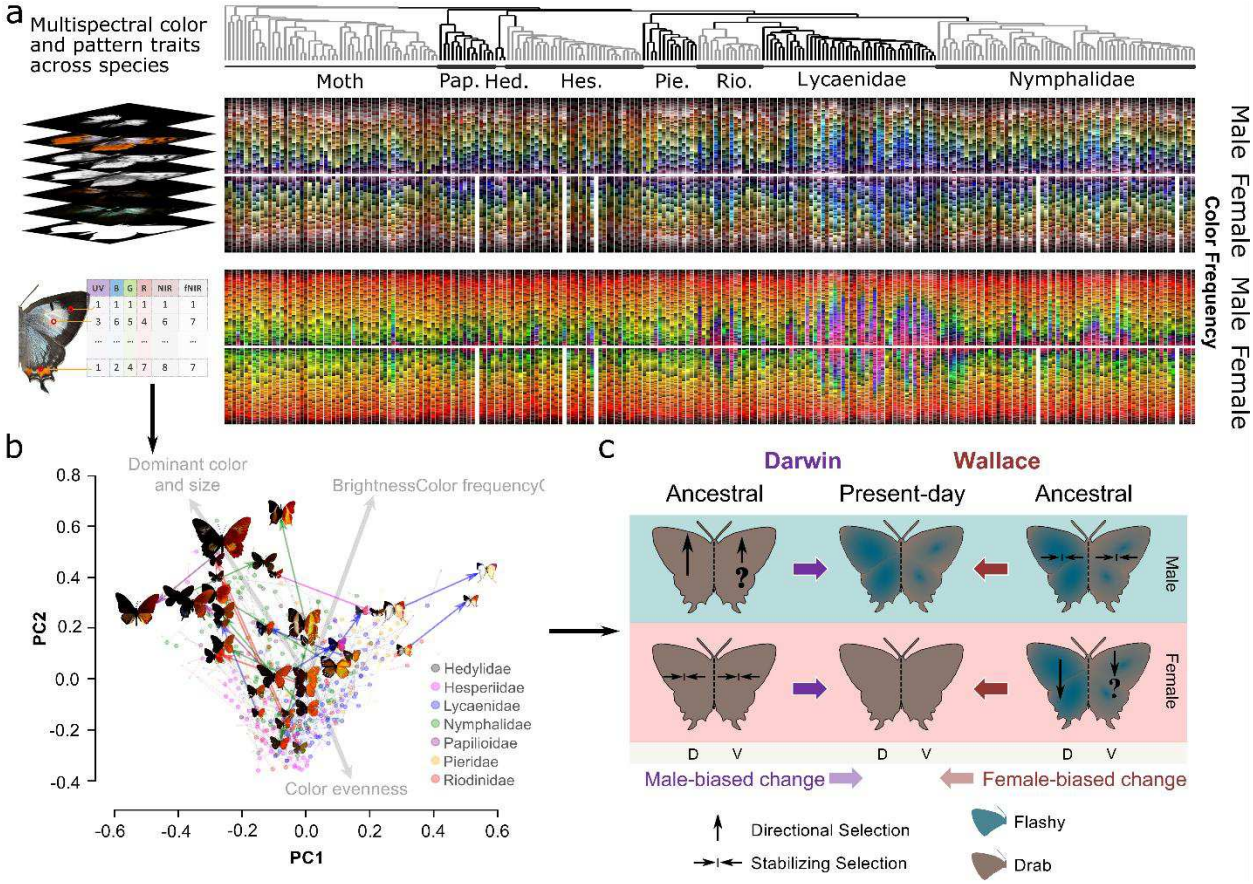

Figure 1: **Quantifying macroevolutionary patterns of sexual bias to test Darwin's and Wallace's hypotheses.** **A)** Left: 240 multispectral reflectance and pattern traits were extracted from wavelength-band imaging[18] of specimens (image stack), including various measures of pattern complexity (e.g. spectral heterogeneity, Kolmogorov complexity) across the wing as well as multispectral 'color palette' trait metrics (inset table showing three different 'multispectral colors' from which color diversity statistics such as richness or diversity can be calculated (explained further in Methods). Right: The relative frequency of RGB (top) and false-color (bottom) UV (blue channel)-740 nm (green channel) - 940 nm (red channel) multispectral 'colors' on the dorsal forewings of each species of moth and butterfly used in this study. The size of each block indicates its relative frequency in the wing. Phylogenetic clades are shown in alternating shades to enhance visual contrast. **B)** The 240 traits were subjected to a sensitivity analysis, retaining those relatively unaffected by sampling bias (see Methods, Extended Data Fig. 1), which were then scaled and converted to uncorrelated morphospace axes *via* PCA. Plot. The plot shows species-level dorsal side median values for principal components 1 and 2. Points denote female medians, while lines show

the distance to male medians (tips). The most dimorphic species are visualized, RGB (left wings) and false-color UV-740nm-940nm (right wings). **C)** In Darwin's model (left), males (top) of ancestrally drab species (grey butterflies, left) experience sexual selection for vibrant coloration whereas in Wallace's model, females (bottom) of ancestrally flashy species (blue butterflies, right) experience natural selection for drab coloration, resulting in present-day dimorphism (center). 'D' and 'V' denote dorsal and ventral sides, respectively. A novel workflow uses morphospace axes to calculate whether evolutionary rates and morphological disparity are 'biased' towards (i.e. greater in) males vs females, which are morphological indicators associated with sexual selection (see Extended Data Fig. 2 for calculations).

In this study, we developed a high-throughput, multispectral imaging analysis pipeline (Fig. 1) to investigate the degree to which sexual selection is responsible for sex-specific differences in wing patterns across the Lepidoptera. We first used multispectral wavelength-band imaging[18] to measure 240 multispectral wing reflectance and pattern traits across six wavelength-bands from the ultraviolet (UV) to the near-infrared (NIR) (365-1000 nm) for over 3000 pinned museum specimens of butterflies and moths. These spanned exemplar species from several comprehensive phylogenetic trees including a tribal-level phylogeny of butterflies[19], a superfamily and family-level sampling of Lepidoptera, including many nocturnal moth families[20], and a subfamily and tribal-level phylogeny of the moth family Geometridae, including both day and night-flying species[21]. Following sensitivity analyses, between 185-223 traits remained, which we decomposed into multidimensional reflectance and pattern morphospaces to estimate the relative contribution of sexual selection to each wing surface using three morphological correlates of sexual selection. Finally, we gauged the level of support for sexual selection indicated by these morphological correlates by comparing how well they conform to specific hypotheses about sexual selection on morphological traits (summarized in Table 1). To further address these key hypotheses, we compare findings for butterflies (diurnal, except for Hedylidae) to contexts where we have an *a priori* expectation of reduced sexual selection on visible traits, such as in nocturnal moths, or in wavelength ranges not perceptible to butterflies. We further examine the role of diurnal behavior in explaining the differences we observed between butterflies and moths by comparing day-flying with night-flying moths

in the family Geometridae, an ancestrally nocturnal group with many independent origins of diurnal activity[22].

	Sexual selection prediction	Supporting evidence	Figures, tables
1	*Signal Partitioning: Sexual selection is more pronounced on butterfly dorsal vs. ventral sides*[23,24].	**Strong**- Consistently greater dimorphism on dorsal sides, with greater male bias in butterflies.	Fig. 2, Fig. 3 A-C, ED Fig. 7
2	*Signal Partitioning: Sexual selection is more pronounced on butterfly forewings vs. hindwings*[23,24].	**Moderate**- Reduced male bias on ventral hindwings; male-biased dimorphism correlation reduced on hindwings.	Fig. 2, Fig. 3 A-C, ED Fig. 7
3	*Sensory Drive: Sexual selection is weaker on traits that are harder to perceive by conspecifics*[25].	**Strong**- Dimorphism, male bias significantly reduced in night-flying moths and in wavelength-bands that are not perceptible by butterflies and/or moths.	Fig. 3
4	*Higher correlation between sexually selected traits vs. naturally selected ones*[26,27].	**Strong**- Dimorphic, male-biased traits overlap more in butterflies, especially on dorsal sides.	ED Fig. 6
5	*Higher rates of evolution in sexually vs. naturally selected traits*[26,28].	**Mixed**- Strong positive relationship between dimorphism and rate of evolution in butterflies and moths; butterfly dorsal forewings show positive relationship between male bias and evolutionary rate. Other butterfly wing areas, and wing color traits of nocturnal moths show little or negative relationship (female bias).	Supp. Tables 3-4, ED Fig. 8
6	*More dimorphism in sexually vs. naturally selected traits*[23,29].	**Moderate**- Dimorphism positively correlated with male bias on dorsal sides of butterflies. Negative or no correlation on ventral sides or in nocturnal moths.	ED Fig. 7
7	*Selection increases with transitions to diurnal behavior (extension of sensory drive).*	**Limited-** Dorsal forewing coloration of day-flying Geometridae tends to be more male-biased than that of night-flying geometrids.	Fig. 4

Table 1: Support for hypotheses on patterns of morphological trait evolution under sexual selection. A series of predictions for patterns of morphological evolution under sexual selection from the literature are provided, along with an assessment of the degree to which our data support these predictions. Relevant figures or tables showing results are listed in column 4.

Signatures of sexual selection in traits:

(1847 words)

Comparative studies have employed several signatures of sexual selection quantified directly from male and female morphological traits[27,30,31]. Sexual dimorphism is often considered sufficient evidence of Darwin's model, even though natural selection may also contribute to it[23] (Fig. 1A). Nevertheless, sexual dimorphism commonly results from sexual selection, and studies assessing both types of selection find that sexual selection results in more extreme sexual dimorphism[5,28,29]. Moreover, sexual selection often results in strong directional selection in males[32]. When coupled with stabilizing natural selection in females, clades known to experience widespread sexual selection have shown greater rates of morphological evolution and inter-species morphological disparity in males compared to females (i.e. 'male-bias')[26,27,30,31,33,34]. In contrast, female-biased rates of morphological change expected under Wallace's model (Fig. 1A) are most often observed through processes mediated by natural selection, such as female-limited mimicry[7,10] or cryptic coloration. Thus, these three indicators of sexual selection (dimorphism, male-bias, and interspecific disparity) can provide indirect evidence of sexual selection[26,29], and are particularly useful when combined with additional supporting evidence[35]. Knowledge of a species' perceptual limitations, for example, logically constrains interpretation about the function of traits that vary in perceptibility[36].

The simplest approach to determining male-female differences in traits (i.e. dimorphism) or absolute rate of evolution or morphological disparity is to take the difference between sexes across all species. This analysis reveals a stark difference between butterflies and moths (Figure 2). Where significant differences are detected, butterflies tend to be male-biased in absolute rate of evolution and morphological disparity, while nocturnal moths tend to be female-biased. While most significantly dimorphic or sexually biased butterfly traits do not overlap substantially with those of moths, traits related to color richness, color contrast, reflectance, and overall size (e.g. number of multispectral colors or normalized reflectance in different wavelength bands) overlap substantially more (Extended data Fig. 3). This analysis also recovered the well-documented female size bias across Lepidoptera[23] and recapitulated the general patterns from our global analysis of mostly male-biased traits in butterflies and female-biased traits in

nocturnal moths. However, the differences in units and the correlations between the raw traits in this dataset make it challenging to determine the extent to which sexual selection influences butterfly wing color and pattern traits as a whole.

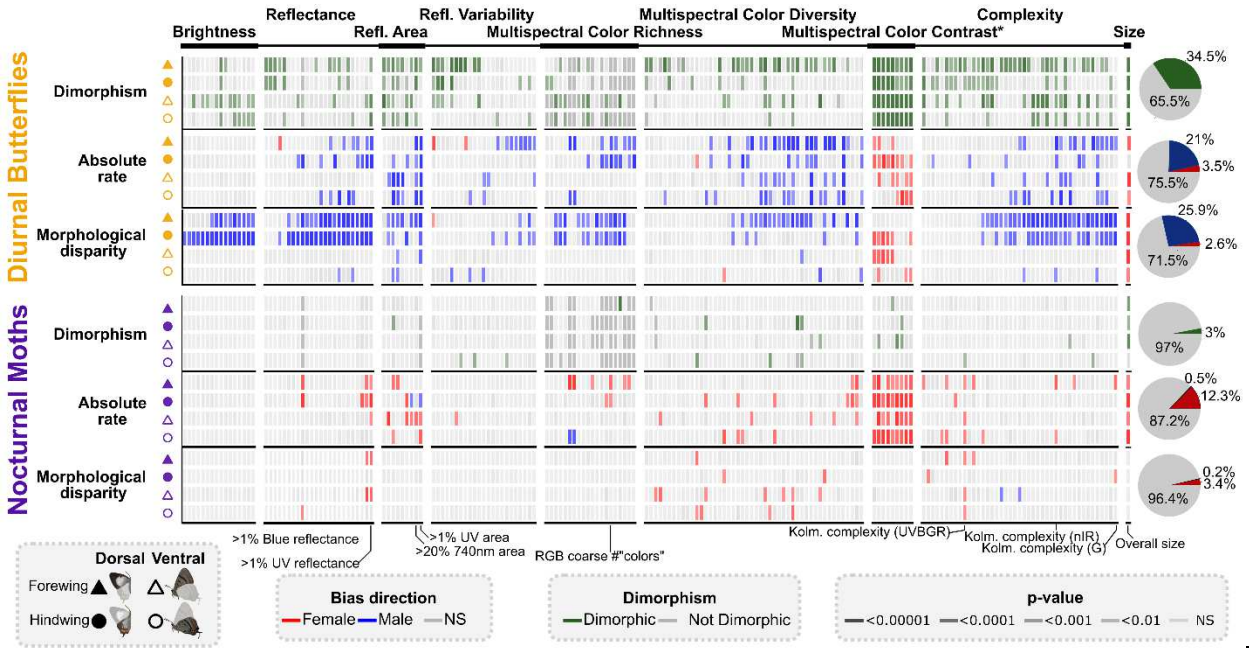

Figure 2: Dimorphism and sexual bias in wing pattern traits of butterflies and nocturnal moths. Each column is a different trait (N = 204) describing wing multispectral colors/patterns within the category indicated at the top. Using all species in the dataset, values were calculated separately for each unique combination of butterfly or moth sides and wings, adjusted with Benjamini-Hochberg's correction[37]. Values for males and females were then compared to each other within each combination to assess dimorphism and bias in absolute rate and morphological disparity. The color intensity of each cell indicates its significance. Red and blue coloration denotes female or male bias, respectively, and green indicates dimorphism. Pie charts show the percentage of significantly dimorphic (green) or significantly male- and female-biased (blue and red) traits across both wings and sides. *The color contrast category contains only raw color contrast, which scales directly with the overall specimen size.

Morphospace indices of Sexual selection:

Previous approaches have used Euclidean distances of individual quantitative traits between males and females to quantify sexual dimorphism and standardize the units of traits (as in Reference 10). Because the axes of our morphospace share the same units, we can similarly use Euclidean distances between

males and females of each species, summed across all axes to quantify the magnitude of overall sexual dimorphism (Extended Data Fig. 4). However, measures of distance cannot be directly compared between butterfly and moth morphospaces. To make these direct comparisons, we expressed mean-squared distances as a proportion of the total morphospace variance, which we call the Absolute Morphological Variance (AMV) dimorphism. This AMV measurement captures all the observed variability between males and females, much of which is idiosyncratic and species-specific.

However, some of the most intriguing examples of dimorphism identified by AMV come from lineages where males and females are broadly similar except for a single iconic morphological feature that the males consistently bear (*e.g.*, enlarged blue dorsal forewing patches in lycaenid males). We thus developed a second measure of dimorphism, the sex Treatment Sum of Squares (TSS) dimorphism, that emphasizes the consistency of group-level dimorphism across all species (Fig. 3A, D).

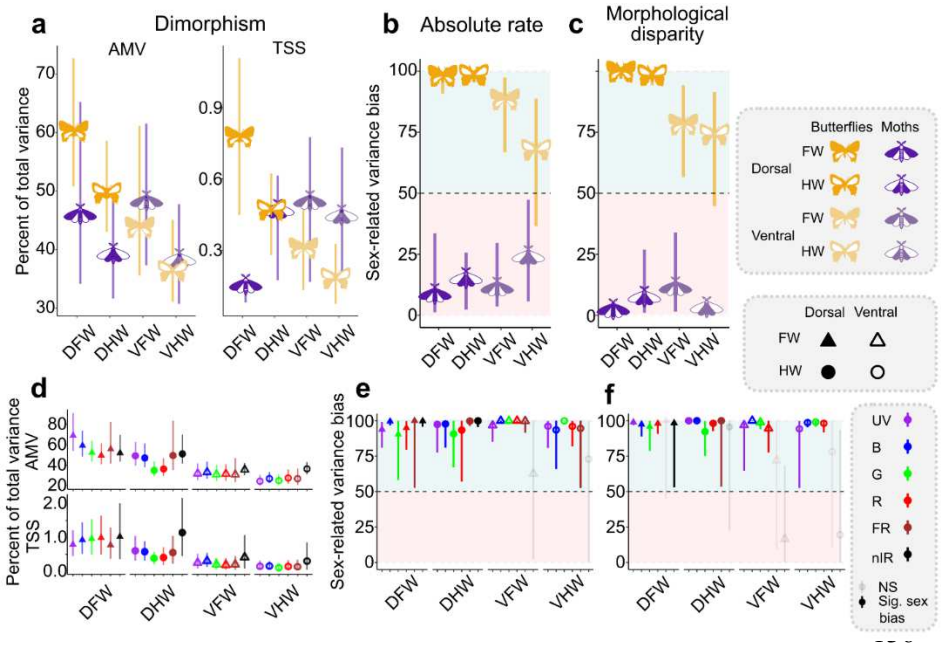

Figure 3: Sexual bias in butterflies supports Darwin's model of sexual selection, while nocturnal moths support Wallace's explanation of female-biased natural selection. (D = dorsal; V = ventral; FW = forewing; HW = hindwing) Sexual dimorphism and male-bias in the absolute rate of evolution and morphological disparity were used to identify patterns consistent with sexual selection in the morphospaces of butterflies and moths. **A)** Absolute Morphological Variance (AMV) and the Treatment Sum of Squares (TSS) Sexual dimorphism measures in the forewings and hindwings of butterflies and moths, dorsally and ventrally, expressed as a percent of total morphospace variance for each wing and side. **B-C)**

Percentage of male-biased to total sex-related variance across both wings and sides in the absolute rate of evolution **(B)** and morphological disparity **(C)**, indicator metric formulas described in ED Fig. 2. **D-E)** Dimorphism **(D)**, absolute rate **(E),** and morphological disparity **(F)** plotted separately for different single wavelength-bands. Error bars represent bootstrapped 95% confidence intervals (see Methods), while points show the median values of the full dataset.

Testing hypotheses of sexual selection:

To probe the link between male bias and sexual selection, we explored whether patterns of dimorphism and sexual bias varied predictably in contexts where *a priori* differences in the degree of sexual selection on wing traits were expected (Table 1). In the following sections, we explore these hypotheses in detail:

Both Darwin and Wallace originally speculated that the potential for mate-signaling should be on the dorsal surfaces, while the ventral surfaces are primarily for crypsis to avoid predators[38,39] (Hypotheses 1-2, Table 1). This theory was later expanded to include differences between hindwings and forewings because hindwings are partially hidden while at rest, and thus will experience weaker natural selection. As a result, potentially antagonistic signaling functions like predator avoidance and mate signaling can potentially be partitioned into different surfaces. In support of this 'Signal Partitioning Hypothesis'[24], We found that evidence for sexual selection is indeed stronger on the dorsal and forewing surfaces of butterflies than the ventral and hindwing surfaces (hypotheses 1-2, Table 1), as demonstrated by the higher AMV and TSS dimorphism measurements (Fig. 3A, right). In addition, males show significantly faster evolutionary rates and greater morphological disparity than females, on both sides of the forewings and the dorsal hindwings (Fig. 3B and C, top), but no male bias was detected on the less visible ventral hindwings. Taken together, these findings support a Darwinian model of sexual selection as the primary driver of color and pattern evolution in butterflies on their dorsal and forewing surfaces. While it is possible that faster male trait evolution could be driven in males by more intense natural selection rather than sexual selection, this explanation seems less likely: It would require explaining why sex-specific natural selection produces such a pronounced male bias, and why it should be greatest in the dorsal and

166 forewing areas when natural selection is expected to be greater relative to sexual selection in the ventral
167 and hindwing areas[23,24].

168 Endler's 'Sensory Drive' hypothesis[25] (Hypothesis 3, Table 1) stipulates that less perceptible traits should
169 experience less effective sexual selection. We thus hypothesized that sexual selection on wing color and
170 pattern traits should be reduced or even absent among less visually-oriented nocturnal taxa, and in
171 wavelength-bands not perceptible to butterflies (hypothesis 3, Table 1). Nocturnal moths provide an ideal
172 system to test this because they heavily rely on pheromones for sexual signaling[40], and their superposition
173 eyes reduce visual acuity in exchange for increased light sensitivity at night. These features suggest that
174 visually-mediated signaling should be less effective in moths, though the role of sexual selection in
175 shaping color and patterning in the wings of nocturnal moths remains largely unexplored (but see
176 Reference 41).

177 To test this hypothesis, we assessed sexual differences in nocturnal moth wing patterns. We found that
178 though moths have comparable levels of overall (AMV) sexual dimorphism as butterflies, they have
179 significantly less consistent (TSS) dimorphism in their dorsal forewings, suggesting that dorsal forewing
180 dimorphism is more variable in its directionality across nocturnal moth species (Fig. 3A). Moreover, their
181 absolute rate of evolution and morphological disparity are significantly female-biased in all contexts (Fig.
182 3B-C). These patterns suggest the role of sex-specific natural selection on female wing color and pattern
183 traits, such as for defensive coloration (crypsis or aposematism) to compensate for the increased predation
184 risk of larger female body sizes[23]. Female-biased evolutionary rates and morphological disparity in
185 nocturnal moths could also be caused by male choice acting on female wing traits, but this seems unlikely
186 given their nocturnal habit, widespread reliance on pheromonal communication for mate-signaling and
187 the relative rarity of male choice compared to female choice[23] in the Lepidoptera.

188 We further tested the Sensory Drive hypothesis by analyzing patterns of dimorphism and sexual bias in
189 'butterfly-visible' (UV, blue, and green; red for butterflies with red receptors) vs 'butterfly-invisible' (740
190 and 940 nm NIR) single-wavelength-band morphospaces. Butterfly-visible bands were male-biased in

nearly all contexts, especially in the ultraviolet, where sexual signaling is well documented[12–15]. In contrast, male bias is either absent or more variable in the NIR wavelength bands, especially in the 940nm band which is well beyond documented lepidopteran sensitivity (Fig. 3E-F). Sexual differences in the 940nm band are much less correlated with those in any other wavelength band in general (0.33 mean R^2 compared to 0.52 for other bands, Extended data Fig. 5), even though UV-visible and NIR reflectivity are often highly correlated in natural spectra[42]. This could indicate a reduced impact of sexual selection and/or a greater contribution of naturally selective pressures such as thermoregulation (as NIR wavelengths represent a substantial solar energy flux[43]), and reflection of NIR wavelengths (known to confer thermal protection in birds and butterflies[42,44]).

While the 740nm nIR wavelength band exhibits similar patterns to those of the 940 nm nIR band, they appear much less pronounced than might be expected. A likely explanation is that 740nm reflectance is highly correlated with reflectance in the red band (Extended data Fig. 5), a correlation also known from other natural spectra[42]. Therefore, sexual selection targeting the red band would also affect 740 nm features through indirect selection of functionally-linked traits. In addition, a few butterfly species are known to be able to perceive wavelengths beyond 700nm[45,46]. The ability to perceive this range by some species could be particularly useful given its invisibility to vertebrate predators and its greater transmission through dense forest canopies. If more species of butterflies can utilize 740nm light for signaling, this might also explain the differences between the patterns we observed in the 740 and 940 nm wavelength ranges. Further work is needed to investigate the ability of Lepidoptera to detect and respond to far-red light to resolve these questions.

Different indices of sexual selection in traits are often correlated with each other[1,47,48]: We expected relatively greater correlation among these indices when driven by sexual selection compared to natural selection (Hypothesis 4, Table 1). The analysis of dimorphism and sexual bias of individual morphospace axes for butterflies and moths strongly supports this expectation: We grouped axes into six categorical groupings based on whether they have either above or below average AMV dimorphism, or are male- or

female- biased in absolute rate and morphological disparity. We found that on the dorsal forewings of butterflies, where our findings and those of previous researchers suggest they should experience the strongest sexual selection (Table 1), most morphological axes are in the category with above average AMV dimorphism and male-biased absolute rates of evolution and morphological disparity (Extended data Fig. 6). In contrast, in contexts where we expect less sexual selection, such as on the ventral sides, hindwings, or in the traits of nocturnal moths, most axes are in mixed categorical groupings thatshow contrasting patterns of dimorphism or sexual bias (Extended data Fig. 6).

The rate of evolution and magnitude of dimorphism tend to be greater in sexually selected vs. naturally selected traits[28,29]. We therefore predicted that more male-biased morphological axes should also evolve faster or be more sexually dimorphic (Hypotheses 5-6, Table 1). However, linear modeling of relationships between dimorphism and male bias in absolute rates and morphological disparity (as an indication of sexual selection) found only modest support for correlations between sexual dimorphism and male bias (ED Fig. 7). Absolute male-female morphological variance (AMV) shows a significant positive relationship with male bias in morphological disparity and absolute rate of evolution on the dorsal wings of butterflies (Table S2). Neither index of sexual bias is significantly correlated with consistent group-level male-female TSS. In contrast, AMV dimorphism is correlated with female bias in both indices in the ventral wings of nocturnal moths and with morphological disparity bias in butterfly ventral hindwings (ED Fig. 7) (Table S2).

The predictions of the Sensory Drive Hypothesis and our findings of the drastic contrast between patterns of sexual bias in primarily diurnal butterflies and nocturnal moths suggest that transitions to diurnal behavior may be associated with increased sexual selection on visible wing traits in the Lepidoptera (Hypothesis 7, table 1). However, diurnal activity is thought to have evolved only once in butterflies and reverted in the small family Hedylidae (three species of which were included in our butterfly analyses, though removing them did not meaningfully change the results, File S3)[22]. The relationships between traits and diurnal activity in butterflies are therefore potentially confounded by shared ancestry. To

address this concern, we applied our analysis to the moth family Geometridae, where day-flying behavior has evolved multiple times within an ancestrally nocturnal group[22]. We analyzed a subset of 23 strictly day-flying and 25 strictly night-flying geometrids sampled from across a recent comprehensive geometrid phylogeny[21] (though the smaller sample sizes precluded single wavelength-band or individual trait-level analyses).The phylogeny was calibrated using divergence time estimates from Reference 21 as calibration points, due to the lack of abundant Geometridae fossils. We also verified the robustness of our results that rely on these divergence time estimates by performing an additional analysis that does not rely on branch-length scaling (Fig. 4D).

Differences between day-flying and night-flying geometrids were more subtle than between butterflies and our broader sampling of nocturnal moths. However, on their dorsal sides and specifically their forewings, day and night flying geometrids exhibit differences in sexual dimorphism and sexual bias similar to those found in our broader analysis of diurnal butterflies vs. nocturnal moths: Though day-flying geometrids had substantially lower Absolute Morphological dimorphism on all wings and sides, they show a trend for much greater dimorphism that was consistent across species (TSS, Fig. 4A) and show significant male bias in morphological disparity and absolute rate of evolution on their dorsal forewings (Fig. 4C).

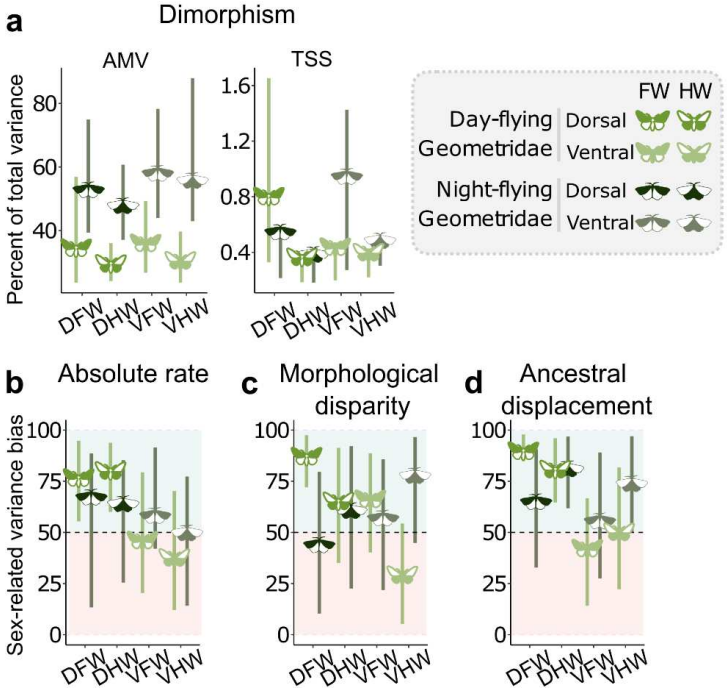

Figure 4: Signatures of sexual selection in the dorsal and forewing areas of day-flying Geometridae. A) Sexual dimorphism and **B-C)** Percentage of male-biased to total sex-related variance across both wings and sides in the absolute rate of evolution and morphological disparity, as described in Figure 3. **D)** As noted in the text, we also used a branch length-independent measure of ancestral change to further support the

absolute rate patterns we derived from our time-calibrated Geometridae phylogeny. These are also expressed as male bias in the sum of squared variances across all day or night flying species variances, plotted as a proportion of the total sex-related variance. Error bars represent the bias-corrected accelerated bootstrap 95% confidence intervals from 100,000 bootstraps (Methods), while points show the median values of the full dataset.

Absolute rate of evolution was also more male biased on the dorsal hindwings of day-flying species vs. night-flying species (Fig. 4B). In contrast, night-flying geometrids do not show any significant sexual biases in absolute rates or morphological disparity. On the ventral side, there was a high degree of variability and no significant differences between day- and night-flying moths in sexual dimorphism measured by TSS, or sexual biases in absolute rates and morphological disparity (Fig. 4). This may be due to more recent transitions to diurnality in the geometrids, which only arose as a family ~80 Mya[22].

Taken together, these patterns suggest that transitions to diurnal behavior may amplify sexual selection pressures on dorsal wing surfaces, especially forewings, despite the strong but highly variable sexual dimorphism that night-flying species exhibit.

Darwin vs. Wallace:

Overall, we find evidence of strong sexual selection on wing color and patterns in clades, wing surfaces and wavelength bands expected to follow Darwin's model: on the dorsal forewings of day-flying butterflies in wavelengths that their eyes can see. Evidence for sexual selection on wing color and patterns is weak or absent in night-flying moths, and in wavelengths that butterflies cannot detect. Furthermore, the stronger male biases in dorsal forewing areas in day-flying geometrids suggests that transitions to day-flying behavior (likely mediated by changes to visual processing and signaling) may be associated with this increased sexual selection and that these effects are strongest in the dorsal forewings and hindwings. This similarity to butterflies occurs even though, unlike most butterflies, day-flying geometrids rarely close their wings at rest and thus natural and sexual selection may not segregate between dorsal and ventral sides in the same way that they do in butterflies[24].

Our analysis assesses broad-scale trends in sex-specific lepidopteran wing patterns. Not all predictions from previous studies align completely with the patterns we observed, and different clades vary in male-female dimorphism and male bias in their morphological evolution. Many individual butterfly clades or wing traits clearly bear the mark of natural selection, as in the case of female-limited mimicry in *Papilio*[7], or in the thermally beneficial high-altitude melanism of female *Colias philodice eriphyle,* despite being disfavored by males[8]. However, in our comprehensive analysis, across exemplars representing nearly all butterfly tribes using correlates of sexual selection that integrate across a wide array of wing color and pattern traits, we find that dimorphism in butterflies is overwhelmingly more consistent with Darwin's explanation of sexual selection than Wallace's explanation of natural selection. In contrast, in nocturnal macro-moths, which show strong but highly variable sexual dimorphism and highly female-biased patterns of evolution, we find the reverse is true. We also consistently find in both butterflies and day-flying geometrid species that ventral and hindwing surfaces, where both Darwin and Wallace speculated that natural selection might predominate, reduced or absent signatures of sexual selection.

Our analysis in geometrid moths of the possible role of diurnal flight habit in explaining differences between day and night-flying species broadly echoed these differences. Though less clear cut, we found that, similar to butterflies, day-flying geometrids show consistent dimorphism and significant male bias in morphological disparity specifically in their dorsal forewings. Further research in other groups where these transitions have occurred over a range of time periods will help to clarify effects on dimorphism, disparity, and rates of morphological evolution in males and females. But overall, these findings suggest a link between transitions to diurnal behavior and increased sexual selection in these wing areas.

Author contributions:

Conceptualization: R.A.R.C., W.P.C., J.D.C, M.A.C, N.E.P.; **Methodology**: R.A.R.C. ,W.P.C., S.M., B.V.D., W.V.M., A.S., J.D.C, M.A.C, G.D.B., C.C.T., R.H.S., C.A.M, M.C.S., E.R.S., N.Y., N.E.P.; **Software**: .A.R.C., W.P.C., V.S., V.B., E.R.S., R.G., L.R.; **Formal Analysis**: R.A.R.C., W.P.C., L.C., S.A., B.V.D., N.E.P.; **Investigation:** R.A.R.C., W.P.C., L.C., S.A., S.M., J.H., M.G.I., E.D.; **Resources**: K.A.P., A.P.S.C, J.F.R.T, A.O., R.V., G.T., C.C.T., D.P., E.F.A.T., R.H.S., C.A.M., J.H., M.G.I., V.S., V.B., G.D.B., M.C.S., E.R.S., M.E., R.G., W.J., A.K.K., D.J.L., L.R., N.Y., N.E.P.; **Writing- original draft**: R.A.R.C., W.P.C., B.V.D., D.J.L., N.Y., N.E.P.;

Writing-review & editing: all authors. **Visualization**: R.A.R.C., W.P.C., B.V.D., N.E.P.; **Project administration**: R.A.R.C., W.P.C., S.M., R.H.S., C.A.M, R.G., W.J., A.K.K., D.J.L., L.R., N.Y., N.E.P.; **Funding acquisition**: R.G., W.J., A.K.K., D.J.L., L.R., N.Y., N.E.P.

Data availability:

All raw data and intermediate data products are available from the Harvard Dataverse (https://doi.org/10.7910/DVN/WUYCRG). Catalog numbers for specimens used in this study are included in file S2.

Code availability:

A walkthrough of the following analysis is available at https://github.com/astaroph/Multispectral-sex-selection-walkthrough, with generalized code that can be easily adapted by each user. The specific scripts used in the analyses are available from the Harvard Dataverse (https://doi.org/10.7910/DVN/WUYCRG).

Acknowledgments:

We thank Jay Goldberg, Sixing Chen, Julien Ayroles, and Patrick Gemmel for helpful suggestions on drafts of this paper. The high-performance cluster at Harvard University provided computational support. Funding was provided by the US National Science Foundation (NSF) GoLife 'ButterflyNet' collaborative grant (DEB-1541500, 1541557, 1541560) to A.Y.K., R.P.G., D.J.L. and N.E.P as well as an NSF Physics of Living Systems grant (no. PHY-1411445) awarded to N.Y. and N.E.P, and an NSF Graduate Research Fellowship Program fellowship to R.A.R.C..

References:

1. Shultz AJ, Burns KJ. The role of sexual and natural selection in shaping patterns of sexual dichromatism in the largest family of songbirds (Aves: Thraupidae). Evolution. 2017;71(4):1061–74.
2. Cooper I, Brown J, Getty T. A role for ecology in the evolution of colour variation and sexual dimorphism in Hawaiian damselflies. Journal of Evolutionary Biology. 2016;29(2):418–27.
3. Seehausen O, Mayhew P, Van ALPHEN J. Evolution of colour patterns in East African cichlid fish. Journal of Evolutionary Biology. 1999;1(2):514–34.
4. Shine R. Ecological causes for the evolution of sexual dimorphism: a review of the evidence. The Quarterly Review of Biology. 1989;64(4):419–61.
5. Dunn PO, Armenta JK, Whittingham LA. Natural and sexual selection act on different axes of variation in avian plumage color. Science advances. 2015;1(2):e1400155.
6. Van der Bijl W, Zeuss D, Chazot N, Tunström K, Wahlberg N, Wiklund C, et al. Butterfly dichromatism primarily evolved via Darwin's, not Wallace's, model. Evolution Letters. 2020;
7. Kunte K. Mimetic butterflies support Wallace's model of sexual dimorphism. Proceedings of the Royal Society B: Biological Sciences. 2008;275(1643):1617–24.
8. Ellers J, Boggs CL. The evolution of wing color: male mate choice opposes adaptive wing color divergence in *Colias* butterflies. Evolution. 2003;57(5):1100–6.
9. Hoyal Cuthill JF, Guttenberg N, Huertas B. Male and female contributions to diversity among birdwing butterfly images. Communications Biology. 2024;7(1):774.
10. Puissant A, Chotard A, Condamine FL, Llaurens V. Convergence in sympatric swallowtail butterflies reveals ecological interactions as a key driver of worldwide trait diversification. bioRxiv. 2023;2023–02.
11. Lukhtanov VA, Kandul NP, Plotkin JB, Dantchenko AV, Haig D, Pierce NE. Reinforcement of pre-zygotic isolation and karyotype evolution in *Agrodiaetus* butterflies. Nature. 2005;436(7049):385–9.
12. Robertson KA, Monteiro A. Female *Bicyclus anynana* butterflies choose males on the basis of their dorsal UV-reflective eyespot pupils. Proceedings of the Royal Society B. 2005;272(1572):1541–6.
13. Kemp DJ. Female butterflies prefer males bearing bright iridescent ornamentation. Proceedings of the Royal Society B: Biological Sciences. 2007;274(1613):1043–7.
14. Papke RS, Kemp DJ, Rutowski RL. Multimodal signalling: structural ultraviolet reflectance predicts male mating success better than pheromones in the butterfly *Colias eurytheme* L.(Pieridae). Animal Behaviour. 2007;73(1):47–54.
15. Kemp DJ, Rutowski RL. Condition dependence, quantitative genetics, and the potential signal content of iridescent ultraviolet butterfly coloration. Evolution. 2007;61(1):168–83.

16. Munro JT, Medina I, Walker K, Moussalli A, Kearney MR, Dyer AG, et al. Climate is a strong predictor of near-infrared reflectance but a poor predictor of colour in butterflies. Proceedings of the Royal Society B. 2019;286(1898):20190234.
17. Kang C, Im S, Lee WY, Choi Y, Stuart-Fox D, Huertas B. Climate predicts both visible and near-infrared reflectance in butterflies. Cleo Bertelsmeier, editor. Ecology Letters [Internet]. 2021;24(9):1869–79. Available from: https://doi.org/10.1111/ele.13821
18. Chan W-P, Childers RR, Ashe S, Tsai C-C, Elson C, Keleher KJ, et al. A high-throughput multispectral imaging system for museum specimens. Communications Biology [Internet]. 2022;5(1). Available from: https://doi.org/10.1038/s42003-022-04282-z
19. Espeland M, Breinholt J, Willmott KR, Warren AD, Vila R, Toussaint EF, et al. A comprehensive and dated phylogenomic analysis of butterflies. Current Biology. 2018;28(5):770–8.
20. Kawahara AY, Plotkin D, Espeland M, Meusemann K, Toussaint EF, Donath A, et al. Phylogenomics reveals the evolutionary timing and pattern of butterflies and moths. Proceedings of the National Academy of Sciences. 2019;116(45):22657–63.
21. Murillo-Ramos L, Brehm G, Sihvonen P, Hausmann A, Holm S, Ghanavi HR, et al. A comprehensive molecular phylogeny of Geometridae (Lepidoptera) with a focus on enigmatic small subfamilies. PeerJ. 2019;7:e7386.
22. Kawahara AY, Plotkin D, Hamilton CA, Gough H, St Laurent R, Owens HL, et al. Diel behavior in moths and butterflies: A synthesis of data illuminates the evolution of temporal activity. Organisms Diversity & Evolution. 2018;1–15.
23. Allen CE, Zwaan BJ, Brakefield PM. Evolution of sexual dimorphism in the Lepidoptera. Annual Review of Entomology. 2011;56:445–64.
24. Oliver JC, Robertson KA, Monteiro A. Accommodating natural and sexual selection in butterfly wing pattern evolution. Proceedings of the Royal Society oB: Biological Sciences. 2009;276(1666):2369–75.
25. Endler JA. Signals, signal conditions, and the direction of evolution. The American Naturalist. 1992;139:S125–S153.
26. Friis G, Milá B. Change in sexual signalling traits outruns morphological divergence across an ecological gradient in the post-glacial radiation of the songbird genus Junco. Journal of Evolutionary Biology. 2020;33(9):1276–93.
27. Knapp A, Knell R, Hone D. Three-dimensional geometric morphometric analysis of the skull of Protoceratops andrewsi supports a socio-sexual signalling role for the ceratopsian frill. Proceedings of the Royal Society B. 2021;288(1944):20202938.
28. Martin MD, Mendelson TC. Changes in sexual signals are greater than changes in ecological traits in a dichromatic group of fishes. Evolution. 2014;68(12):3618–28.
29. Safran R, Flaxman S, Kopp M, Irwin DE, Briggs D, Evans MR, et al. A robust new metric of phenotypic distance to estimate and compare multiple trait differences among populations. Current Zoology. 2012;58(3):426–39.
30. Knell RJ, Naish D, Tomkins JL, Hone DWE. Sexual selection in prehistoric animals: detection and implications. Trends in Ecology & Evolution. 2013;28(1):38–47.

31. Cooney CR, Varley ZK, Nouri LO, Moody CJ, Jardine MD, Thomas GH. Sexual selection predicts the rate and direction of colour divergence in a large avian radiation. Nature Communications. 2019;10(1):1–9.
32. Andersson M. Sexual selection. In: Sexual Selection. Princeton University Press; 2019.
33. Prum RO. Phylogenetic tests of alternative intersexual selection mechanisms: trait macroevolution in a polygynous clade (Aves: Pipridae). The American Naturalist. 1997;149(4):668–92.
34. Emlen DJ, Marangelo J, Ball B, Cunningham CW. Diversity in the weapons of sexual selection: horn evolution in the beetle genus *Onthophagus* (Coleoptera: Scarabaeidae). Evolution. 2005;59(5):1060–84. Available from: https://doi.org/10.1111/j.0014-3820.2005.tb01044.x
35. Safran RJ, Scordato ES, Symes LB, Rodr'\iguez RL, Mendelson TC. Contributions of natural and sexual selection to the evolution of premating reproductive isolation: a research agenda. Trends in Ecology & Evolution. 2013;28(11):643–50.
36. Su S, Lim M, Kunte K. Prey from the eyes of predators: Color discriminability of aposematic and mimetic butterflies from an avian visual perspective. Evolution [Internet]. 2015;69(11):2985–94. Available from: https://doi.org/10.1111/evo.12800
37. Benjamini Y, Hochberg Y. Controlling the false discovery rate: a practical and powerful approach to multiple testing. Journal of the Royal Statistical Society: series B (Methodological). 1995;57(1):289–300.
38. Wallace AR. Darwinism: An Exposition of the Theory of Natural Selection, with Some of Its Applications. Vol. 1. Macmillan; 1889.
39. Darwin C. The descent of man: and selection in relation to sex. John Murray, Albemarle Street.; 1888.
40. Hansson B. Olfaction in lepidoptera. Experientia. 1995;51(11):1003–27.
41. Kelley JL, Tatarnic NJ, Schröder-Turk GE, Endler JA, Wilts BD. A dynamic optical signal in a nocturnal moth. Current Biology. 2019;29(17):2919–25.
42. Medina I, Newton E, Kearney MR, Mulder RA, Porter WP, Stuart-Fox D. Reflection of near-infrared light confers thermal protection in birds. Nature Communications. 2018;9(1):3610.
43. Kochevar IE. Photophysics, photochemistry and photobiology. Dermatology in General Medicine. 1987;
44. Tsai C-C, Childers RA, Shi NN, Ren C, Pelaez JN, Bernard GD, et al. Physical and behavioral adaptations to prevent overheating of the living wings of butterflies. Nature Communications. 2020;11(1):1–14.
45. Arikawa K, Pirih P, Stavenga DG. Rhabdom constriction enhances filtering by the red screening pigment in the eye of the Eastern Pale Clouded yellow butterfly, *Colias erate* (Pieridae). The Journal of Experimental Biology. 2009;212:2057–64.
46. Liénard MA, Bernard GD, Allen A, Lassance J-M, Song S, Childers RR, et al. The evolution of red color vision is linked to coordinated rhodopsin tuning in lycaenid butterflies. Proceedings of the National Academy of Sciences. 2021;118(6):e2008986118.
47. Chakrabarty P, Davis MP, Smith WL, Baldwin ZH, Sparks JS. Is sexual selection driving diversification of the bioluminescent ponyfishes (Teleostei: Leiognathidae)? Molecular Ecology 2011;20(13):2818–34.

48. Watanabe A, Fabre A-C, Felice RN, Maisano JA, Müller J, Herrel A, et al. Ecomorphological diversification in squamates from conserved pattern of cranial integration. Proceedings of the National Academy of Sciences [Internet]. 2019;116(29):14688–97. Available from: https://doi.org/10.1073/pnas.1820967116
49. Pennell MW, Eastman JM, Slater GJ, Brown JW, Uyeda JC, FitzJohn RG, et al. geiger v2. 0: an expanded suite of methods for fitting macroevolutionary models to phylogenetic trees. Bioinformatics. 2014;30(15):2216–8.

Extended data:

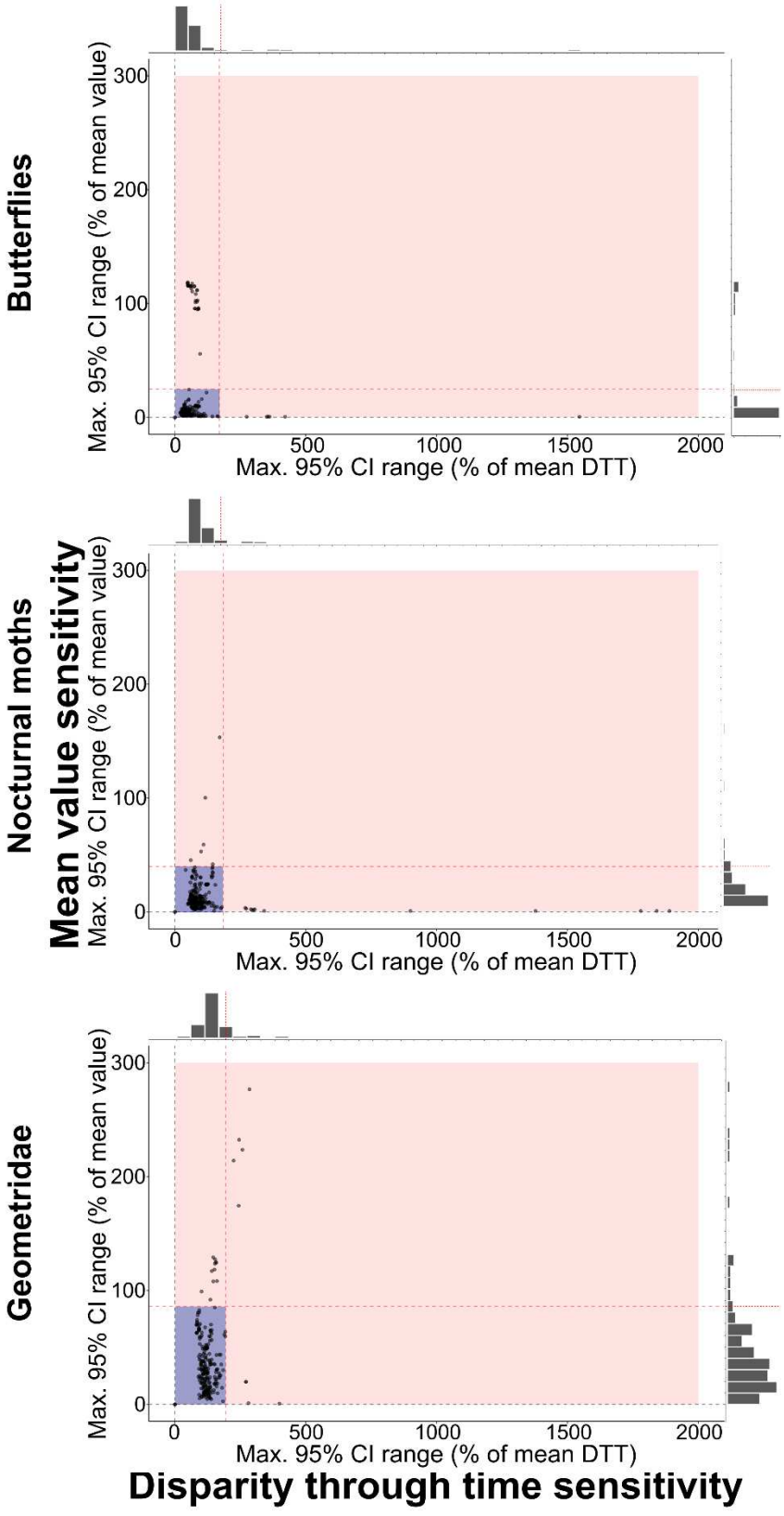

Extended Data Fig. 1: Sensitivity analysis of butterfly, nocturnal moth and Geometridae trait datasets . Bootstrapping was used to determine the sensitivity of trait metrics to sampling bias by comparing the variability in resampled mean (y axes above) and disparity through time[49] (x axes above) values across bootstraps. The range of the 95% confidence intervals of these bootstrap values, expressed as a percentage of the original dataset mean value was calculated for each original trait for each wing (fore- and hind- wing, left and right) and each side (ventral and dorsal) of male and female nocturnal moths, Geometridae and butterfly exemplars. Separately for all datasets, the maximum values across all wings and sides of these values were plotted as histograms (strip charts above) and thresholds in these histograms were determined through visual

inspection (the 'elbow method') to exclude traits with means or patterns of disparity through time that are particularly sensitive to sampling effects (shaded in pink above). Retained traits used in all subsequent analyses are shaded in blue above.

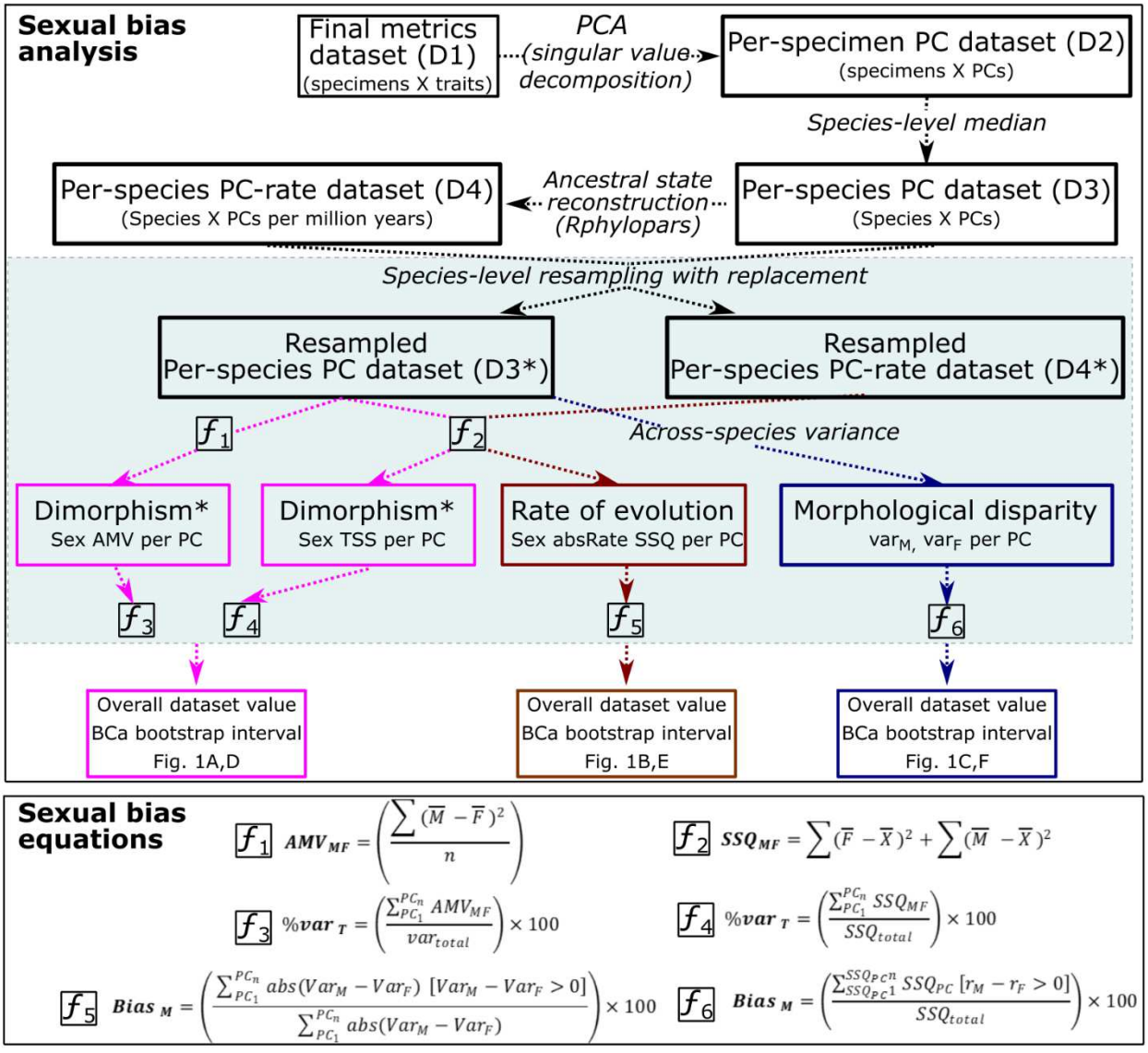

Extended Data Fig. 2: Calculations for quantifying macroevolutionary patterns of sexual bias. Top) Sexual bias analysis. Beginning with a final specimen x trait dataset (D1; post-sensitivity analyses), PCA generates a specimen x principal components dataset (D2). Taking the species-level medians produces a species x Principal Components (PC) dataset (D3). Using a time-calibrated phylogeny, ancestral states are reconstructed for each PC across the tree to produce a species x change in PCs per million years (D4) dataset. D3+D4 are then used to

calculate overall sexual dimorphism and male bias in the absolute rate of evolution and morphological disparity, bootstrapping 100,000 times, resampling species with replacement to generate Bias-corrected and accelerated confidence intervals. **Bottom) Sexual bias equations:** Sexual dimorphism, expressed as sex-related morphological variance relative to the total dataset variance, is calculated in two ways: F1 calculates the Absolute Morphological Variance (AMV), equivalent to the average squared difference between males and females across all species, which measures sexual dimorphism regardless of its direction (greater in males or females), and F2 calculates the male-female Treatment Sum of Squares (TSS) variance, similar to ANOVA group-level means difference testing, measuring sexual dimorphism that is consistent in direction across species, calculated separately for each PC, then summed across PCs to denote the overall sex related morphological variance relative to total dataset variance (F3, and F4). F2 similarly calculates TSS variance for males and females for the absolute rate of evolution.Sex-related morphological disparity variance is calculated as the difference in group-level variance between males and females across all species. Male bias in absolute rate and morphological disparity are then calculated (F5 and F6, respectively) by separately summing variance for PCs where males have higher absolute rates or morphological disparity, and then expressing this value as a percentage of total sex-related variance. See Methods for additional statistical details.

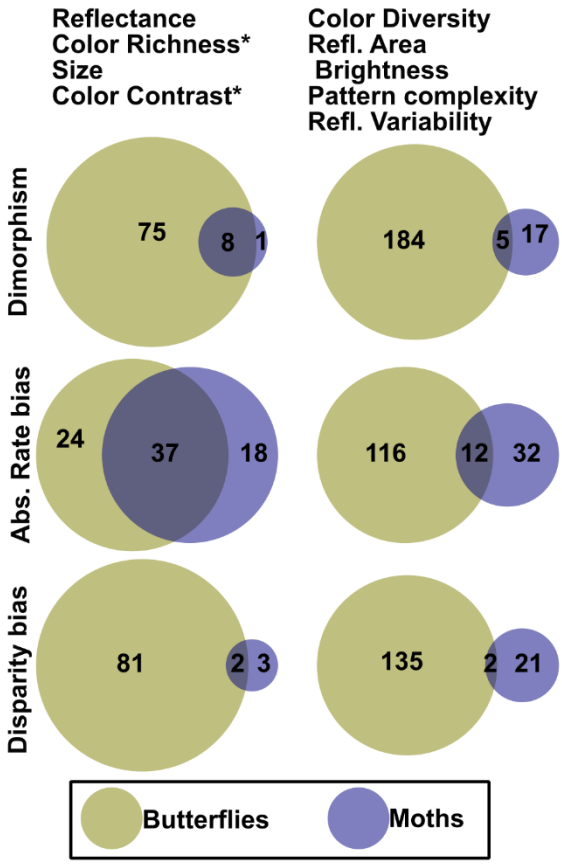

Extended Data Fig. 3: Overlap between nocturnal moth and butterfly indices of sexual selection in different trait categories. Venn diagrams showing overlap between the significantly dimorphic or sex biased traits of butterflies and nocturnal moths from Extended Data Figure 5 across two sets of trait categories. Significant butterfly and nocturnal moth traits related to reflectance, color richness and contrast or overall size show substantially more overlap than those in other trait categories. Venn diagrams were created using DeepVenn (Hulsen, 2022). *Raw color contrast and richness traits were many of the ones found to be significant in this analysis, and scale proportionally with body size.

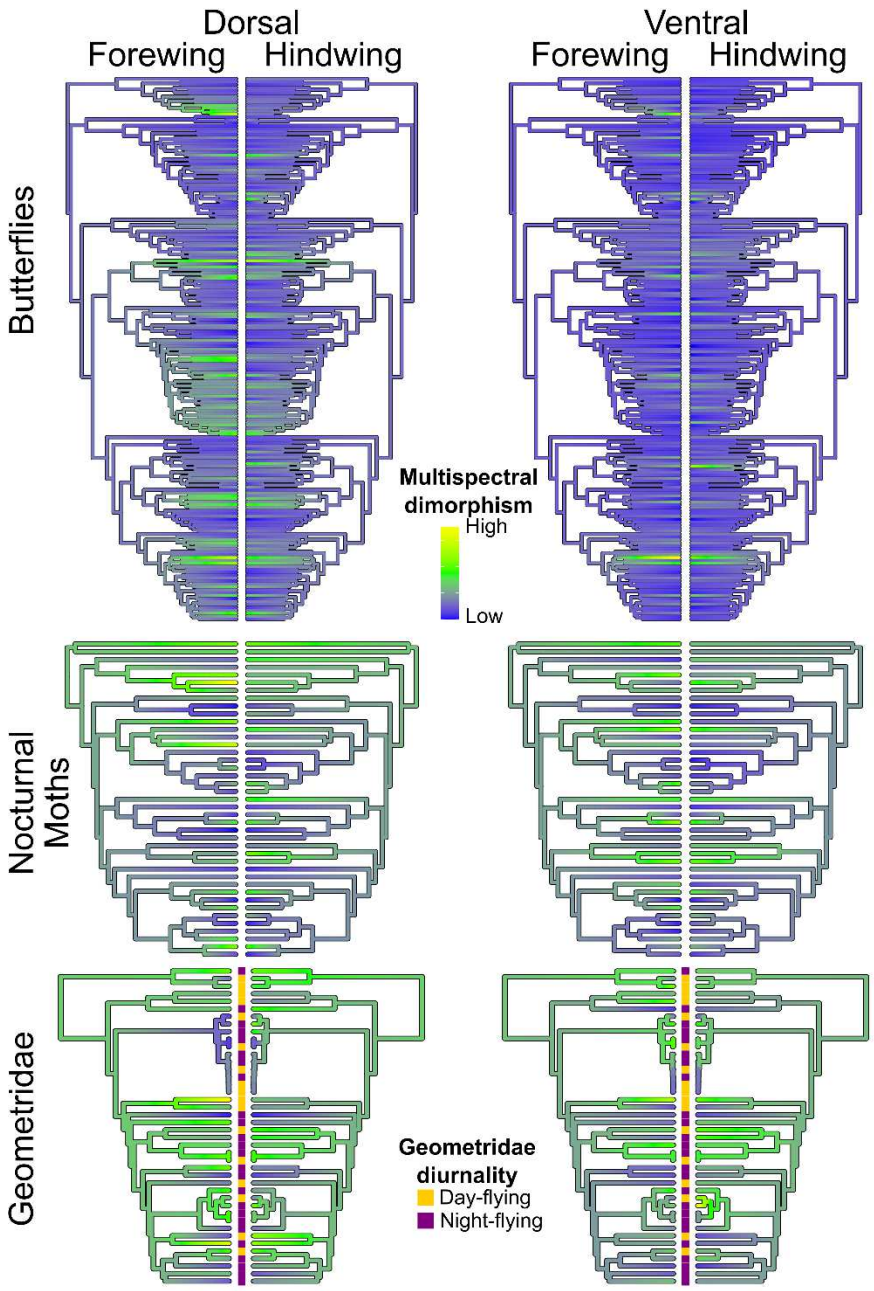

Extended Data Fig. 4: Male-female multispectral dimorphism on the wing surfaces of butterflies, nocturnal moths, and day and night-flying Geometridae. Overall sexual dimorphism calculated across all the wing surfaces of the butterflies and moths is mapped onto the Espeland et al. (2018) phylogeny of butterflies, the subsets of 41 species of nocturnal moths from the Kawahara *et al*. (2019) phylogeny and 42 day and night-flying exemplar species from the Murillo-Ramos *et al.* (2019) phylogeny of Geometridae. This dimorphism represents the Euclidean distance between males and females across all axes in each morphospace, denoted "Multispectral dimorphism," which is then scaled to compare relatively high or low levels of dimorphism between morphospaces and mapped onto the phylogenies above using Brownian motion ancestral state reconstruction for visualization (Methods). The Murillo-Ramos *et al.* (2019) phylogeny has been time-calibrated using published divergence time estimates as described in the Methods.

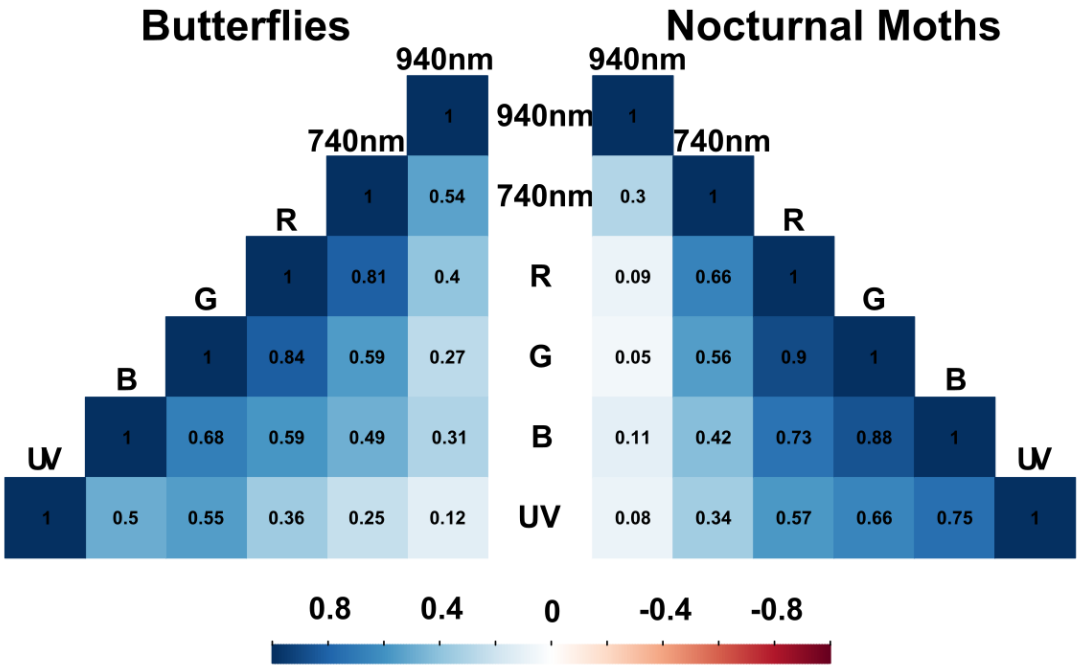

Extended Data Fig. 5: Phylogenetically corrected linear relationships between dimorphism distance in different wavelength bands. Phylogenetically corrected linear relationships were produced by using the 'pglmm' function in the phyr package in R (Ives *et al.* 2020) to model the linear relationships between male-female Euclidean distances in different wavelength bands. Values displayed above are analogous to Pearson correlation coefficients between dimorphisms in different wavelength bands after differences between dorsal/ventral and forewing/hindwing dimorphism have been taken into account by including 'Side' and 'Wing' as fixed effects in the models, though not on a strict -1,1 scale due to the influence of the random effects structure of the models, see Methods.

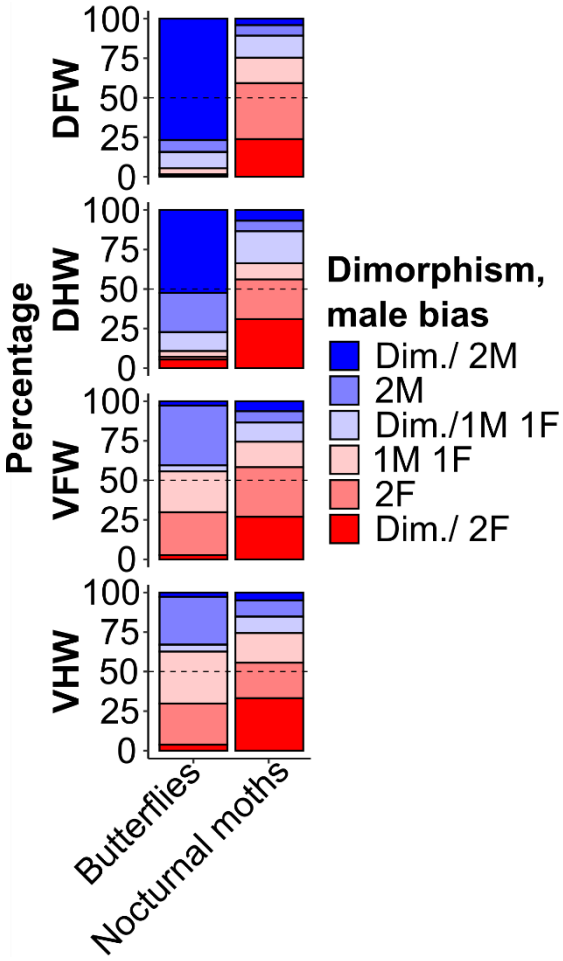

Extended Data Fig. 6: Patterns of overlapping sexual bias and dimorphism in indices of sexual selection across wing surfaces of exemplars from butterfly and nocturnal moth phylogenies. Stacked barplots show the percentage of morphological axes (individual PCs) that overlap in their patterns of Dimorphism (Absolute Morphological Variance), absolute rate of evolution and morphological disparity bias. Groups of traits with above average dimorphism are denoted as "Dim." in the legend entries, whereas male or female bias in absolute rate or morphological disparity is denoted as "M" or "F," respectively with "1" or "2" denoting whether one or both of these indices is male or female biased for that group of traits. DFW: 'Dorsal Forewing,' DHW: 'Dorsal Hindwing,' VFW: 'Ventral Forewing,' VHW: 'Ventral Hindwing.' Dashed lines denote the 50% of all morphological axes. More axes show overlapping patterns of male bias and dimorphism in the dorsal and forewing surfaces of butterflies than in their hindwing or ventral surfaces or in the wings of nocturnal moths, where dimorphic traits tend to be female-biased.

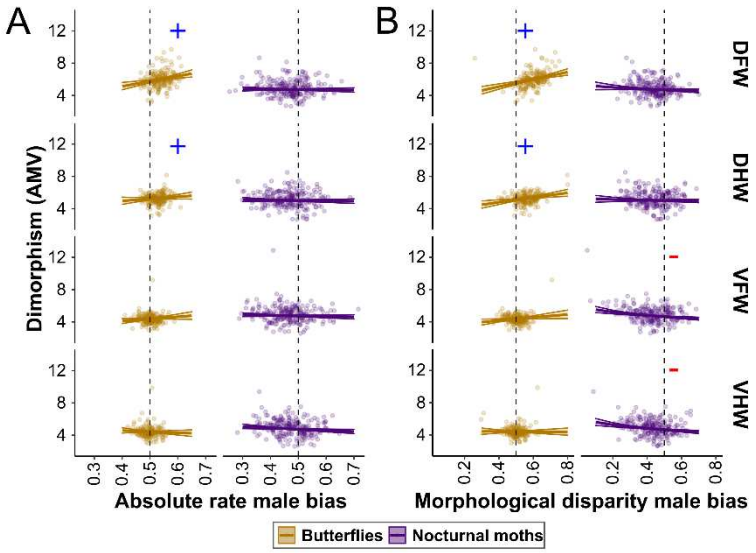

Extended Data Fig. 7: Relationships between indices of sexual selection in butterflies and nocturnal moths. The individual principal component axes of the butterfly or nocturnal moth morphospaces were used to study the relationship between Absolute morphological variance (AMV) dimorphism, and male bias in either absolute rates (**A**), or morphological disparity (**B**). Points represent relative values for individual principal components from their respective morphospaces. Linear relationships between AMV dimorphism and both bias indices were explored using separate mixed effects linear models for each taxon, with significant positive or negative relationships in these models denoted by blue plus or red minus signs, respectively, with no annotation indicating no significant relationship (see Methods for statistical model details). Confidence envelopes representing the fixed effects confidence intervals of a model fit across all taxa together are included for visualization purposes. Model output included in Table S2.

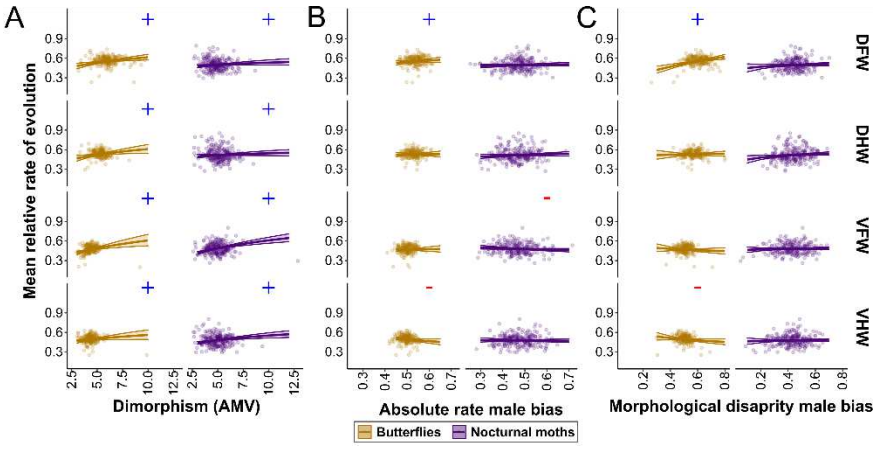

Extended Data Fig. 8: Relationships between absolute rate of evolution and indices of sexual selection in butterflies and nocturnal moths. The individual principal component axes of the butterfly or nocturnal moth morphospaces were used to study the relationship between the average (across males and females of all species) absolute rate of evolution and the absolute morphological variance (AMV) dimorphism (**A**) or male bias in either absolute rates (**B**), or morphological disparity (**C**). Points represent relative values for individual principal components from their respective morphospaces. Linear relationships between the average rate of evolution and the proxies of sexual selection were explored using separate mixed effects linear models for each taxon, with significant positive or

negative relationships in these models denoted by blue plus or red minus signs, respectively, with no annotation indicating no significant relationship. 95% Confidence envelopes representing the fixed effects confidence intervals of a model fit across all taxa together are included for visualization purposes. See Methods for statistical modeling details. Model output included in Table S2.

Supplementary data table. 1: Description of trait metrics created and used

Supplementary data table 2: Emmeans slope significance testing output for butterflies and nocturnal moths average rate, dimorphism, sexual bias linear model analysis

Supplementary data table 3: Calibration points and references for timetree calibration of Geometridae phylogeny

Supplementary data file 1: Time calibrated Geometridae phylogeny in Newick format. Species names are ordered tip numbers matching the original phylogeny in Murillo-Ramos *et al.* (2019)

Supplementary data file 2: Catalog numbers and metadata of butterfly and moth specimens used in this study.

Supplementary data file 3: Overall and singleband sexual selection indicator analysis for butterflies excluding three night-flying Hedylidae species

Supplementary data file 4: Determinations and justifications for Geometridae diurnal behavior activity pattern categorizations.

Methods

Data collection and generation of primary reflectance metrics

Specimen selection, sampling and imaging

Up to 6 male and 6 female specimens were selected for each exemplar species in a tribal-level phylogeny of butterflies[1] (1168 male and 1020 female specimens total, 185 out of 195 tips representing > 90% of all butterfly tribes). If we were unable to locate sufficient specimens for a particular species (or subspecies), another species in the genus (or subspecies) was analyzed. A total of 2,188 butterfly specimens were examined from the Museum of Comparative Zoology, Harvard University, and the McGuire Center at the Florida Museum of Natural History, University of Florida. Similarly, 160 female and 216 male specimens of 41 nocturnal moth species were sampled from a phylogeny of all Lepidoptera based on full transcriptomes and genomes[2]. 57 male and 61 female specimens of 23 day-flying and 25 night-flying Geometridae moth species were also sampled as exemplars from a comprehensive geometrid phylogeny[3]. A table of catalog numbers for each specimen used in this study is included in file S2. For each species, I used the iNaturalist 'browse-photos' tool to look at Research Grade observations' photos, and evaluated presence/absence of significant, repeated evidence of 1) daytime activity in the sun, 2) daytime activity in the shade, 3) daytime resting behavior, 4) nighttime attraction at artificial light sources, and 5) other night-time activity. Based on these scores, we designated each species as "Day-active only (often in the sun)", "Night-active only", "Night- and day-active", "Day-active only (only at twilight or in the shade)", "Night- and twilight- or shade-limited day-active", or "data deficient." We only considered species that appeared active either at night or day, but not both, in further analyses. See File S4 for a detailed description of these determinations made for each species used in the study.

A custom-built, high-throughput imaging system and analysis pipeline was designed to conduct multispectral imaging of the dorsal and ventral sides of each specimen and extract multispectral reflectance traits from individual specimen images, which used both built-in optional supervision and manual correction steps to perform background removal, fore- and hindwing segmentation, and produce linearized measures of reflectance (albedo) for the dorsal and ventral sides of both forewings and hindwings[4].

Geometridae phylogeny time-calibration, morphological displacement from ancestors

Comprehensive time-calibrated phylogenies are not currently available for the family Geometridae. We therefore performed our own time-calibration of the phylogeny from Reference 3, using published divergence time estimates available on timetree.org [2,5–8]. We compiled a list of divergence points spread throughout the phylogeny, excluding those with estimated time ranges that were too broad, or which diverged sharply across studies. We provided the average minimum and maximum ranges for 17 remaining calibration points to the makeChronosCalib and chronos functions of the ape package in R (version 4.2.2 was used for all analyses) for making time-calibrated phylogenies (provided with references in Table S3). We tested both relaxed and correlated models of evolution and a range of lambda values, selecting the best-fitting tree via log likelihood. We tested the fit of this tree using a separate set of 3 divergence points intentionally left out of the time calibration, estimating the mean percent error between each point and its predicted divergence in our best fitting tree (<2% for the final tree, Supplementary file 1). We used this tree in all subsequent analyses of absolute rate of evolution in the Geometridae dataset.

We also conducted an equivalent analysis to complement our absolute rate of evolution analysis that does not rely on branch lengths, estimating morphological displacement from ancestral values. In this analysis, we simply calculated the trait value difference between each tip and its

most recent ancestor. As with the absolute rate calculation, we calculated the male-female treatment sum of squared variance of these ancestral differences across all PCs, summing male biased and female biased PC variances separately to calculate an overall proportion male bias across all PCs, which produced broadly similar results to the absolute rate analysis (Fig. 4D).

Reflectance-based metrics

The measures of reflectance used were reflectance (0-1), reflective area (cm^2) and reflectance variability (coefficient of variation), as previously described in Reference 4. These were calculated separately for subsets of pixels at a range of reflectance thresholds (0, 0.05, 0.1, 0.2) which exhibited qualitatively distinct patterns: relating to either overall reflectance across the entire wing surface (0, 0.05 thresholds) or only brightly colored wing patches which exhibited particularly strong reflectance (0.1, 0.2 thresholds). Multispectral reflectance was further summarized in the average reflectance across different combinations of wavelength bands (i.e. overall specimen brightness), as well as in Kolmogorov complexity scores (compressed:uncompressed image size ratio[9]) for each wavelength band and across different wavelength band ranges. Additionally, we used Principal components analysis to summarize higher-dimensional patterns of reflectance across the 6 wavelength bands (UV, B, G, R, 740nm, 940nm) into the top 3 principal components (explaining 41.9%, 22.0% and 13.0% percent of the total variability, respectively), either globally (across all pixels in the dataset) or locally (within the pixels in a single image), which could be used for false-color visualizations of reflectance or for calculating the Kolmogorov complexity of reflectance variance itself. See Supplementary Data Table 1 for full description of specific reflectance traits.

Primary analysis

Color palette metrics

To quantify higher-order aspects of multi-spectral 'coloration' and patterning, we developed additional metrics to quantify the abundance, diversity, evenness, and entropy of "multispectral color classes" on the wings, derived from combining reflectance values across multiple wavelength band combinations (Figure 1A). Specifically, we developed a 'multi-spectral reflectance palette' by converting the 255-level intensity values of each raw wavelength band (UV, B, G, R, 740nm and 940nm) image into 8 equally sized intensity levels, plus a zero. Concatenating these values across all wavelength bands yields a unique categorical label, which we refer to, for convenience, in the remainder of this manuscript as a 'multi-spectral color,' though these labels are not defined relative to any visual system. This vastly reduced color palette (531,441 versus 2.75 $x10^{14}$ 'colors') made it computationally tractable to use the frequency and spectral and spatial distributions of these 'multispectral colors' to quantify metrics such as Shannon-Weaver entropy and evenness, the spatial extent of these 'multispectral colors' across the wing as well as overall 'multispectral color' diversity and contrast, for each wing and body part separately. We also calculated the Moment-Distance Index, which quantifies the shapes of color-frequency distribution histograms with a single value, often employed by other wavelength-band imaging systems such as remote sensing applications[10] . This can be thought of as a numeric descriptor of wing color diversity and utilization. For a complete description of all the metrics we developed, see Supplementary Data Table 1. Calculations were done in Python (3.7.4)[11] using core packages 'itertools,' 'sys,' 'time,' 'collections,' 'pickle,' 'logging,', 'optparse,' and 'math'[11], as well as the Pandas (1.1.3)[12,13], Numpy (1.16.5)[14], Scipy (1.4.1)[15], Scitkit-klearn (0.21.2)[16], Logging (0.5.12) and Optparse (1.5.3) modules.

Sensitivity analyses and final trait datasets

To account for the effect of sampling bias in these exemplar datasets, we conducted sensitivity analyses on each trait: We examined the variability across subsamples in 1) the overall trait mean and, to incorporate a measure of how bias affected evolutionary patterns, 2) through the variability in the trait disparity through time[17]. Specifically, male and female specimens across each entire dataset were randomly resampled with replacement 10,000 times. For each combination of forewing/hindwing, dorsal/ventral, male/female, species-level mean and disparity through time values were calculated for the species present in all datasets. 95% percentile confidence intervals of these values were calculated for each dataset, yielding 8 ranges expressed as percentages of the original mean (one for each wing, side, and sex). The maximum of these 8 values for mean value and disparity through time was plotted (Extended Data Figure 1), and breakpoints in the sensitivity of traits to sampling bias across these two dimensions were identified using the elbow method (dashed lines in Extended Data Figure 1). Traits below these elbow thresholds were retained for subsequent analyses. Sensitivity analyses were run separately for butterfly, nocturnal moth, and geometrid datasets. We ultimately retained 185, 223, and 222 traits in the final butterfly, nocturnal moth, and Geometridae datasets, respectively (Extended data Fig. 1).

Construction of the final trait datasets and morphospaces and morphological axes

We only retained species that contained at least one male and one female specimen each. Separately for butterflies and moths, data across wings, sides and sexes were scaled and then jointly decomposed into butterfly and moth 'morphospaces' via principal components analysis in Python (3.7.4)[11]: datasets were first mean-centered and scaled to unit variance across all wings, sides and sexes using the StandardScaler function from the SciKit learn package (1.2.2)[16], and then decomposed via singular vector decomposition into uncorrelated 'morphological axes' (e.g. Fig. 1B) using the PCA function from the Scikit-learn package.

Overall sexual selection indices analysis

A key property of our morphospaces, which are produced by singular vector decomposition performed on traits that are mean centered and scaled to unit variance, is that distances and variances are directly comparable across morphospace axes. This allowed us to express three indices of sexual selection as variances: (1) sexual dimorphism, (2) male bias in the absolute rate of evolution and (3) group level morphological disparity. These were then summed across the uncorrelated singular vectors of our morphospaces to produce summary values for sexual dimorphism or male bias across all traits on each wing and side. We explain the process for calculating these variances or male bias values for each index of sexual selection in detail below.

Dimorphism: The simplest calculation of overall sexual dimorphism across multiple different traits that share the same unit space is Euclidean distance (as in Reference 18). However, unitless distances cannot be compared between different PCA morphospaces, so in order to directly compare the magnitude of sexual dimorphism across all butterfly and moth datasets, we express squared Euclidean distances as a function of the overall morphospace variance, producing a variance which scales with the magnitude of overall sexual dimorphism between males and females and which we refer to the as the Absolute Morphological Variance (AMV).

This measure of dimorphism scales with increasing male-female differences, regardless of the direction of these differences. Thus, regardless of whether male-female trait differences change in direction between species, the species as a group will still exhibit a high AMV. However, a key component of Darwin's model for the origin of sexual dimorphism in butterflies was that sexual selection resulted in *consistently* flashier males. Thus, we developed an index that scales with consistent sexual dimorphism across species: the sum of squared differences between male and female species medians, across all species, for each principal component in our morphospaces. These are then summed across all morphospace axes to produce the

overall sex-related sum of squares, analogous to the between-treatment variance of an Analysis of Variance. We plotted these (in Figures 3A and 4A, along with AMV dimorphism) as a percentage of total dataset variance to produce a quantitative estimate of how large sexual dimorphism was relative to overall morphological variability that is comparable across morphospaces.

Absolute rate of evolution sexual bias: To calculate the sexual bias in the absolute rate of evolution, we first derived ancestral state values, which can be divided by the branch length to yield a rate of evolution. Specifically, the absolute rate of evolution was calculated by using the Rphylopars package in R[19] to reconstruct ancestral state values for each principal component across each butterfly, nocturnal moth, or geometrid phylogenetic tree. For each reconstruction, we tested five different evolutionary models (Brownian, Early-Burst, Orstein-Uhlenbeck, lambda, and kappa) proceeding with the one that fit best via AIC. Rates of trait change across each branch were calculated by taking the difference between parental and descendant nodes or tips and dividing these differences by the branch lengths, producing a rate of change per million years. To minimize the uncertainty inherent in estimating the ancestral values of deep nodes, we only used the rates of change from each species tip to their immediate parental nodes. We then calculated the sum of squared (SSQ) differences between the male and female absolute rates for each principal component. To determine the overall level of sexual bias across all principal components, we summed these sex-related SSQ differences across all axes that had higher male absolute rates of evolution separately, then plotted the sex-related SSQ values that had higher absolute rates of evolution in males as a percentage of total sex-related SSQ for each side, wing and sex separately (Figure 3B and 3B).

Morphological disparity sexual bias: To calculate the sexual bias in morphological disparity, we utilized the dispRity function from the dispRity package in R[20] to calculate the male and female across species trait variance for each principal component. We then subtracted female

variance from male variance across all components, yielding the sex-related variance, and summed variances in principal components that were greater in males than females (male-biased morphological disparity variance), expressing this value as a percentage of total sex-related variance for each side, wing and sex separately (Figure 3C and 3C).

Bootstrapping and confidence intervals: We randomly resampled species and re-calculated these dimorphism and bias values 100,000 times, as implemented by the boot package in R[21,22], and calculated the bias-corrected accelerated[22] confidence values employing a modified boot.pval function from the boot.pval package in R[23]. P-values were corrected following the method of Benjamini and Hochberg[24].

Extended analysis

Individual trait-level sexual selection indices analysis

In order to examine dimorphism and sexual bias in specific traits, we computed our indices of sexual selection (dimorphism, sexual bias in the absolute rate of evolution and morphological disparity) as male-female differences, allowing for comparison against a null hypothesis of 0 for significance testing for each trait. As a measure of dimorphism, we used the median male-female difference for each species. For male bias in the absolute rate of evolution, we used the median male absolute rate, expressed as a proportion of the sum of median male and female absolute rates. For male bias in morphological disparity, we divided the male trait variance across species (calculated by the dispRity function of the disparity package in R[20]) by the sum of male and female trait variances. As in the global analysis, we employed bootstrap resampling using the 'boot' package[21,22] to calculate bias corrected confidence intervals[22] for these values. From these we derived p-values using a modified version of the 'boot.pval' function of the 'boot.pval' package[24] with a null hypothesis of either zero male-female differences (for

dimorphism) or male absolute rates and trait variance of 0.5 out of 1 (for absolute rates and morphological disparity), corrected via Benjamini and Hochberg (1995).

Individual morphospace axis-level sexual selection indices analysis

To examine the relationship between dimorphism or the average rate of evolution and male bias in absolute rates or morphological disparity, we repeated our individual trait level analysis for individual morphospace axes, adding the absolute morphological variation between males and females across species for each individual PC axis in addition to the male-female differences, as well as the median absolute rate of evolution across both males and females. These axes are uncorrelated by definition, and can be considered as a large, statistically independent sample of 'individual traits.' We restricted this analysis of individual axes to only nocturnal moths and butterflies, as the limited number of day- or night- flying species in the Geometridae dataset precluded analysis at this level of granularity.

To determine the degree of correspondence between patterns of dimorphism and male bias, we first examined patterns of overlap in the dimorphism and male bias in absolute rate and morphological disparity across these individual PCs. Within each morphospace, we categorized individual morphospace axes as either dimorphic, if they were above the mean level of dimorphism, or male or female biased if they were above or below 0.5 proportion male bias, respectively. We then further grouped axes into "2M" or "2F" for male or female bias in both absolute rates and morphological disparity indices or "1M 1F" for male bias in one and female bias in the other index. We then examined patterns of overlap in these categories (Dimorphic, 2M, 2F, or 1M1F) graphically (Extended Data Figure 6).

To examine the relationships between these variables while accounting for differences between wings and sides, we conducted linear modeling using the lmer function of the lmerTest package in R[25], Table S2. We used either the average absolute rate or the AMV dimorphism as response

variables, and the proportion male bias in either absolute rate or morphological disparity as a continuous predictor variable. We first tested untransformed, log10 or square root transformations of continuous predictor or response variables selecting the best combinations over via AIC score. We also included Dataset (a categorical variable combining Wing and Side) as well its interaction with either index of male bias. As the PCs decline sequentially in how much variance they explain, to remove this conflating effect and ensure that different PCs were truly 'comparable' with each other we both scaled (but did not mean center) each PC column to unit variance using the scale function in R, as well as included PC order (an ordinal variable denoting the order from PC_1-PC_n) as an additional fixed effect. We then determined whether there were significant positive or negative linear relationships between male bias in either index and AMV dimorphism or the average rate of evolution using the emtrends function of the emmeans package in R[26], denoting significant positive or negative interactions at the individual dataset level with plus or minus signs in ED Figure 7 (for relationships with dimorphism) and ED Figure 8 (for relationships with the average rate of evolution).

Phylogenetically corrected correlations between dimorphism distance in different wavelength bands.

Phylogenetically corrected fixed effects coefficients are displayed in Extended Data Figure 5 were produced by using the 'pglmm' function in the phyr package in R[27] to model the linear relationships between dimorphism distances in different wavelength bands. These coefficients are analogous to pearson correlation coefficients, except that they are not strictly limited to the -1 to 1 range due to the influence of the random effects in the model. Differences between dorsal/ventral and forewing/hindwing dimorphism are taken into account as fixed effects in the models. Both phylogenetic and non-phylogenetic covariance matrices ('tip_id__") were estimated by these models, with "Gaussian" specified as the family. Correlation coefficients

between the different wavelength bands were extracted and plotted as correlograms in Extended data Figure 5 using the 'corrplot' package in R[27] .

Male-female distance dimorphism and phylogenetic visualization

We calculated an index of overall sexual dimorphism for each species in our datasets by summing the Euclidean distance between male and female species means across all axes in our morphospace, which we refer to as "Multispectral dimorphism." These were mapped onto the phylogenies in ED Figure 4 using the 'fastAnc' function of the Phytools package in R (version 0.7.70)[28].

Supplemental methods references:

1. Espeland M, Breinholt J, Willmott KR, Warren AD, Vila R, Toussaint EF, et al. A comprehensive and dated phylogenomic analysis of butterflies. Current Biology. 2018;28(5):770–8.
2. Kawahara AY, Plotkin D, Espeland M, Meusemann K, Toussaint EF, Donath A, et al. Phylogenomics reveals the evolutionary timing and pattern of butterflies and moths. Proceedings of the National Academy of Sciences. 2019;116(45):22657–63.
3. Murillo-Ramos L, Brehm G, Sihvonen P, Hausmann A, Holm S, Ghanavi HR, et al. A comprehensive molecular phylogeny of Geometridae (Lepidoptera) with a focus on enigmatic small subfamilies. PeerJ. 2019;7:e7386.
4. Chan W-P, Childers RR, Ashe S, Tsai C-C, Elson C, Keleher KJ, et al. A high-throughput multispectral imaging system for museum specimens. Communications Biology [Internet]. 2022;5(1). Available from: https://doi.org/10.1038/s42003-022-04282-z
5. Murillo-Ramos L, Chazot N, Sihvonen P, Õunap E, Jiang N, Han H, et al. Molecular phylogeny, classification, biogeography and diversification patterns of a diverse group of moths (Geometridae: Boarmiini). Molecular Phylogenetics and Evolution. 2021;162:107198.
6. Kumar S, Suleski M, Craig JM, Kasprowicz AE, Sanderford M, Li M, et al. TimeTree 5: an expanded resource for species divergence times. Molecular biology and evolution. 2022;39(8):msac174.
7. Wahlberg N, Snäll N, Viidalepp J, Ruohomäki K, Tammaru T. The evolution of female flightlessness among Ennominae of the Holarctic forest zone (Lepidoptera, Geometridae). Mol Phylogenet Evol. 2010;55(3):929–38.
8. Yamamoto S, Sota T. Phylogeny of the Geometridae and the evolution of winter moths inferred from a simultaneous analysis of mitochondrial and nuclear genes. Molecular Phylogenetics and Evolution. 2007;44(2):711–23.
9. Zenil H, Kiani NA, Tegnér J. Methods of information theory and algorithmic complexity for network biology. In: Seminars in cell \& developmental biology. 2016. p. 32–43.
10. Salas EAL, Henebry GM. Separability of maize and soybean in the spectral regions of chlorophyll and carotenoids using the Moment Distance Index. Israel Journal of Plant Sciences. 2012;60(1-2):65–76.
11. Van Rossum G, Drake FL, others. Python reference manual. Vol. 111. Centrum voor Wiskunde en Informatica Amsterdam; 1995.
12. Pandas development team T. pandas-dev/pandas: Pandas. 2020; Available from: https://doi.org/10.5281/zenodo.3509134
13. McKinney W, others. Data structures for statistical computing in python. In: Proceedings of the 9th Python in Science Conference. 2010. p. 51–6.
14. Harris CR, Millman KJ, Van Der Walt SJ, Gommers R, Virtanen P, Cournapeau D, et al. Array programming with NumPy. Nature. 2020;585(7825):357–62.
15. Virtanen P, Gommers R, Oliphant TE, Haberland M, Reddy T, Cournapeau D, et al. SciPy 1.0: fundamental algorithms for scientific computing in Python. Nature methods. 2020;17(3):261–72.
16. Pedregosa F, Varoquaux G, Gramfort A, Michel V, Thirion B, Grisel O, et al. Scikit-learn: Machine learning in Python. the Journal of machine Learning research. 2011;12:2825–30.
17. Pennell MW, Eastman JM, Slater GJ, Brown JW, Uyeda JC, FitzJohn RG, et al. geiger v2. 0: an expanded suite of methods for fitting macroevolutionary models to phylogenetic trees. Bioinformatics. 2014;30(15):2216–8.

18. Puissant A, Chotard A, Condamine FL, Llaurens V. Convergence in sympatric swallowtail butterflies reveals ecological interactions as a key driver of worldwide trait diversification. bioRxiv. 2023;2023–02.
19. Goolsby EW, Bruggeman J, Ané C. Rphylopars: fast multivariate phylogenetic comparative methods for missing data and within-species variation. Methods in Ecology and Evolution. 2017;8(1):22–7.
20. Guillerme T. dispRity: a modular R package for measuring disparity. Methods in Ecology and Evolution. 2018;9(7):1755–63.
21. Canty A, Ripley BD. boot: Bootstrap R (S-Plus) Functions. 2020.
22. Efron B. Better bootstrap confidence intervals. Journal of the American statistical Association. 1987;82(397):171–85.
23. Thulin M. boot.pval: Bootstrap p-Values [Internet]. 2021. Available from: https://CRAN.R-project.org/package=boot.pval
24. Benjamini Y, Hochberg Y. Controlling the false discovery rate: a practical and powerful approach to multiple testing. Journal of the Royal statistical society: series B (Methodological). 1995;57(1):289–300.
25. Kuznetsova A, Brockhoff PB, Christensen RHB. lmerTest package: tests in linear mixed effects models. Journal of statistical software. 2017;82(13).
26. Ives A, Dinnage R, Nell LA, Helmus M, Li D. phyr: Model Based Phylogenetic Analysis [Internet]. 2020. Available from: https://CRAN.R-project.org/package=phyr
27. Wei T, Simko V. R package “corrplot”: Visualization of a Correlation Matrix [Internet]. 2017. Available from: https://github.com/taiyun/corrplot
28. Revell LJ. phytools: an R package for phylogenetic comparative biology (and other things). Methods in Ecology and Evolution. 2012;3(2):217–23.

Supplementary Files

This is a list of supplementary files associated with this preprint. Click to download.

- SupplementaryInformationcombined.docx
- SIGuide.docx